國立臺灣大學獸醫專業學院臨床動物醫學研究所

碩士論文

Institute of Veterinary Clinical Science
School of Veterinary Medicine
National Taiwan University

Master Thesis

尿液血幼素及丙二醛濃度與貓慢性腎病進程之相關性

Correlation between feline urinary hemojuvelin, urinary malondialdehyde, and chronic kidney disease progression

黃化臻

Hua-Chen Huang

指導教授：李雅珍 博士

Advisor: Ya-Jane Lee, Ph.D.

中華民國 111 年 11 月

Novemver, 2022

doi:10.6342/NTU202210133

CONTENTS

doi:10.6342/NTU202210133

doi:10.6342/NTU202210133

doi:10.6342/NTU202210133

中文摘要

在多種腎臟疾病中，鐵代謝的失衡，是造成腎臟疾病惡化的因子。鐵透過多種途徑傷害腎臟組織，其中，氧化壓力是最主要的途徑之一；與鐵堆積及脂質氧化高度相關的鐵依賴性細胞凋亡(ferroptosis)，也已證實與人類和大鼠的腎損傷密切相關。Hemojuvelin 是身體調控鐵平衡的重要因子，其尿中濃度可作為人類急性腎衰竭的早期指標，而慢性腎病的貓其尿中 hemojuvelin 濃度也顯著高於健康者。在大鼠的實驗模型中，腎臟細胞 hemojuvelin 的調控，與腎臟的鐵堆積及組織傷害相關；急性腎損傷會導致腎臟 hemojuvelin 的表現上升，而抑制 hemojuvelin 的切割，則可降低腎臟組織的鐵堆積、並降低腎臟組織的受損程度。然而尿液中的 hemojuvelin 與腎臟氧化壓力的關聯性，以及兩者與貓慢性腎病進程的關聯，目前尚未有相關數據可供參考。

本研究回溯性納入了 2018 一月至 2021 十一月，於台大動物醫院就診的 60 隻慢性腎病貓。並分別以酵素結合免疫吸附分析法(ELISA)，測定其尿中 hemojuvelin 濃度；硫代巴比妥酸反應測試搭配高效液相層析法(HPLC)，測定其尿中脂質氧化指標—malondialdehyde 濃度。兩者皆以尿中肌酸酐濃度作為校正基準，分別得 urine hemojuvelin-to-creatinine ratio (UHCR)及 urine malondialdehyde-to-creatinine ratio (UMCR)。

實驗結果顯示 UHCR 與慢性腎病的惡化顯著相關。90 天內發生慢性腎病惡化者有顯著較高的 UHCR（中位數 54.42 [IQR 25.31, 97.96] $*10^{-7}$ vs. 15.89 [IQR 5.58, 39.55] $*10^{-7}$，p=0.009）。ROC 曲線分析顯示，UHCR 預測 90 天內惡化的最佳臨界值為 47.744$*10^{-7}$；在此臨界值下，預測 90 天內惡化的敏感性及特異性分別為 0.611

doi:10.6342/NTU202210133

和 0.867。以此臨界值為分界，K-M 生存分析顯示 UHCR 較高者，其惡化期間顯著較短（中位數 81 [95% CI, 40-122]天 vs. 556 [95% CI, 246-866]天，p<0.001）。Cox regression analysis 同樣顯示高 UHCR 者有較高的惡化風險（HR 4.337 [95% CI, 1.971-9.545]，p<0.001），且此風險獨立於傳統的腎指標。此外，在線性迴歸模型下，UHCR 與 UMCR 顯著相關，此相關獨立於傳統的腎指標、但與較高的 globulin 有關。然而，UMCR 與慢性腎病惡化間未能發現關聯。

總結來說，UHCR 具有預測貓慢性腎病惡化的潛力，雖然 UMCR 未和病程惡化顯著相關。同時，UHCR 與 UMCR 二者的顯著關聯性，顯示 UHCR 的升高與相關的鐵代謝失衡，與脂質氧化相關。

關鍵詞：慢性腎病、貓、hemojuvelin、malondialdehyde、鐵、氧化壓力

doi:10.6342/NTU202210133

Abstract

Iron dysregulation contributes to multiple types of renal diseases. Iron causes damage to kidneys through several pathways, and many of them related to increased oxidative stress. Specifically, the iron-dependent cell death, known as ferroptosis, is featured by iron accumulation and lipid peroxidation. Ferroptosis is known to correlate closely to kidney injury in human and rats. Hemojuvelin (Hjv), an iron-regulating protein, is shown to be a promising early biomarker for human acute kidney injury (AKI). Meanwhile, the urinary concentration of Hjv elevated significantly in cats with chronic kidney disease (CKD). Regulation of renal cells' Hjv is related to iron accumulation and tissue injury in rats' model. AKI led to Hjv upregulation in kidney tissues, while inhibiting Hjv cleavage can reduce renal injury significantly. However, the relation between urinary Hjv and renal oxidative stress, as well as their relation with CKD progression, has not yet been investigated in feline CKD.

We retrospectively included 60 client-own CKD cats, presented to NTUVH during January 2018 to November 2021. Urinary Hjv concentration was measured by commercial enzyme-linked immunosorbent assay (ELISA) kit. Renal oxidative status was evaluated through urinary malondialdehyde (MDA) concentration, which was measured by thiobarbituric acid reactive substances (TBARS) assay combined with high performance liquid chromatography (HPLC). Both concentrations will be normalized by urine creatinine concentration (urine Hjv-to-creatinine ratio, UHCR; urine MDA-to-creatinine ratio, UMCR).

Our results showed a significant correlation between UHCR and feline CKD progression. Those who progressed within 90 days have significantly higher UHCR (median [IQR], 54.42 [25.31, 97.96] $*10^{-7}$ vs. 15.89 [5.58, 39.55] $*10^{-7}$; p=0.009). ROC analysis showed

doi:10.6342/NTU202210133

the best cut-off for UHCR prediction of 90-day progression was $47.744*10^{-7}$, with sensitivity and specificity of 0.611 and 0.867, respectively. When divided by this cut-off, K-M survival analysis showed a significantly shorter progression-free interval for those with higher UHCR (median [96% CI], 81 [40-122] days vs. 556 [246-866 days], $p<0.001$). Similarly, Cox regression analysis also showed an increased HR for progression in those with higher UHCR (HR 4.337, 95% CI 1.971-9.545; $p<0.001$), which was independent of tradition renal indexes i.e., sCrea and BUN.

UHCR was found significantly correlated with UMCR, which was independent of traditional renal indexes but dependent on serum globulin. There was no significant correlation between UMCR and CKD progression.

To sum up, UHCR predicts CKD progression in cats. On the other hand, no correlation was found between UMCR and feline CKD progression. UHCR correlates significantly with UMCR, indicating UHCR and related iron dysregulation may correlates with lipid oxidation.

Key word: chronic kidney disease, cat, hemojuvelin, malondialdehyde, iron, oxidative stress

doi:10.6342/NTU202210133

List of Figures

doi:10.6342/NTU202210133

List of Tables

doi:10.6342/NTU202210133

Chapter 1 Introduction

Chronic renal disease (CKD) is one of the most prevalence diseases in cats, and have a great impact on their life expectancy [1-4]. However, despite decades long investigation, the mechanism behind feline CKD is still far from well understood. Multiple factors are known to involve in CKD pathogenesis; among them, oxidative stress has long been found to play a central role [5], with iron regulation emerging as a critical factor in human medicine within past few decades [6].

Iron impact on kidney function had been described in various kinds of kidney diseases. Circulating iron associates with unfavorable outcome in patients suffering from or at risk of acute kidney injury (AKI) [6]; meanwhile, dietary iron restriction or iron chelator administration reduced glomerular and tubular-interstitial injury in multiple rats CKD models [6-9]. These deleterious effects of iron are likely resulted from multiple pathways, including direct oxidative stress to cells components; stimulation of inflammatory responses; or triggering cell death [6].

Hemojuvelin (Hjv) is an iron-regulating membrane protein, expressed by multiple organs including liver, skeletal muscles, heart, adipocytes, and kidney [10-12]. When anchoring on cell membrane, it serves as a positive regulator of hepcidin, which is the central iron regulator in animal body [13]. After being cleaved off from cell membrane, the soluble form of Hjv exerts an opposite function i.e. downregulating hepcidin expression [11, 14, 15]. Hepcidin degrades the iron-exporting protein, ferroportin, thus decrease iron release from iron-storing cells ex, macrophages. Overall, membrane-bond Hjv (mHjv) lowers environmental iron concentration, while soluble Hjv (sHjv) do the opposite.

In 2014, a proteomic study identified sHjv as the most significantly elevated iron-

doi:10.6342/NTU202210133

related protein in AKI patients' urine [11]. Later on, Wang et al. [16] and Ko et al. [17] demonstrated that urinary Hjv (uHjv) predict AKI following cardiac surgery. The predictive value of uHjv outstands that of other AKI biomarker, and adding uHjv into established AKI-predicting clinical score significantly improved score predictive ability [17]. The corresponding finding was reported in feline renal disease in 2020, showing that uHjv elevated significantly in cats with CKD, and the concentration went higher in later stage of the disease [18].

The mHjv-hepcidin axis had been found to protect organs against oxidative damage through lowering environmental iron level [11, 19-21]. Malondialdehyde (MDA), one of the most commonly used indicator of lipid oxidation [22], has been reported to decrease with hepcidin treatment in rats' heart undergoing ischemia-reperfusion injury [19]. Also, inhibition of mHjv cleavage help lipid metabolism, indicating a critical role of mHjv on proper lipid handling by cells [21].

Elevated MDA level had been demonstrated in both human [23-27] and feline [28, 29] renal disease. The serum concentration of MDA related with disease severity [25-27], and urinary MDA level predicts renal function deterioration in human AKI [23, 24] and feline CKD (Chang et al. 2021, unpublished data). However, it is currently unknown whether this elevation of MDA is related to Hjv regulation in renal disease.

The aim of this study is to establish the relation between urinary MDA and Hjv in feline CKD. Also, we will look into the predictive value of these two biomarkers for feline CKD progression. As such, we hope to improve our understanding of mechanism behind feline CKD, and identify possible prognostic factors for disease progression.

doi:10.6342/NTU202210133

Chapter 2 Literature review

2.1 Hemojuvelin and renal disease

2.1.1 Iron regulation in renal disease

Iron, a member of transition metal, is able to release or accept electrons relatively easily and participate in oxidation-reduction reactions. This characteristic makes it a vital component of numerous biochemical pathways, which are crucial for normal body function [30]. However, these redox reactions can also generate reactive oxygen species (ROS), causing significant damage to cellular components [6, 30].

Among multiple organs involving in iron regulation, kidney had been found especially vulnerable to iron-mediated injury. These injuries happen through multiple pathways, including direct oxidative stress to renal cells components; stimulation of inflammatory responses; or triggering regulated cell death [6].

Inflammation is the characteristic finding of chronic kidney diseases (CKD), which severity links to renal functional decline in feline CKD [1, 31]. While a wide range of different factors contribute to CKD inflammation, iron had been shown to play a role in it, as low-iron diet decreased inflammasome formation in proteinuric mice model [7]. Two possible mechanisms had been suggested behind this link. First, iron stimulate inflammatory response in macrophages [6], and macrophages is commonly found in kidneys of cats with IRIS stage 2 or more advanced CKD [1]. Meanwhile, in mice injected with iron-dextran solution, iron accumulates mainly inside interstitial macrophages [32]. Together, these findings indicate that iron might participate in CKD inflammation through fueling inflammatory response of interstitial macrophages. On the other hand, kidney cells may itself release inflammatory substances in response to iron stimulation. In human

doi:10.6342/NTU202210133

embryonic kidney cells (HEK 293), the transcription activity of NF-κB, IL-6, and COX-2 had been found to increase significantly when co-incubated with oxidative iron [33].

Another pathway of iron-origin kidney damage is through regulated cell death. Ferroptosis, a nontraditional cell death officially named in 2012, is characterized by intracellular iron accumulation leading to mitochondrial lipid peroxidation [34, 35]. This kind of cell death mainly result from cells' inability to deal with iron-origin oxidative stress, demonstrated by increased oxidative product and impaired antioxidant system. Among several antioxidant systems involved, the glutathione (GSH)- glutathione peroxidase 4 (GPX4) system is thought to be the dominant one [35]. A strong link had been established between ferroptosis and acute kidney injuries (AKI) [6, 34]; ferroptosis is the dominant cell-death form in various AKI models, including folic acid-induced, rhabdomyolysis, and ischemia- reperfusion injury [9, 34, 36]. Meanwhile, GPX4 deletion can lead to spontaneous kidney injury in mice [37]. More recently, a link between ferroptosis and CKD had also been proposed. Wang et al. demonstrated that ferroptosis also involve in 5/6 nephrotomy CKD model, and treatment with iron chelator can significantly ameliorate renal fibrosis through ferroptosis pathway [9].

doi:10.6342/NTU202210133

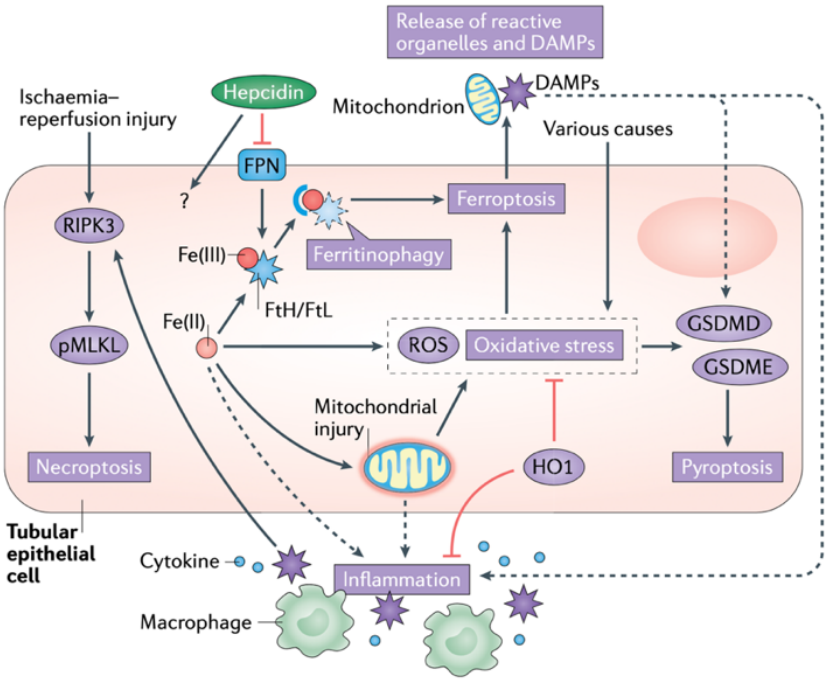

Figure 2-1 Mechanisms of iron-mediated kidney injury and cell death. [6]

Clinically, the impact of iron loading on renal function had been described in human under several medical conditions. Cohort studies in patients with AKI, or at risk of AKI due to cardiac surgery and critical illness, have shown that circulating iron are associated with increased risk of death and renal replacement therapy [6]. Consistently, dietary iron restriction reduced glomerular and tubular-interstitial injury in multiple rats CKD models, as well as iron chelator administration [6-8].

Several diseases had been known to cause increased iron loading, causing iron-origin injuries to organs. Among them, haemochromatosis is one of the most well-known example. The disease is defined by congenital deficiency or resistance of hepcidin, the major negative regulator of body iron balance. Increased level of urinary iron excretion, renal iron deposition, and severe kidney injury had been noted in some of haemochromatosis patients, as well as demonstrated consistently in relevant animal models [38-40].

doi:10.6342/NTU202210133

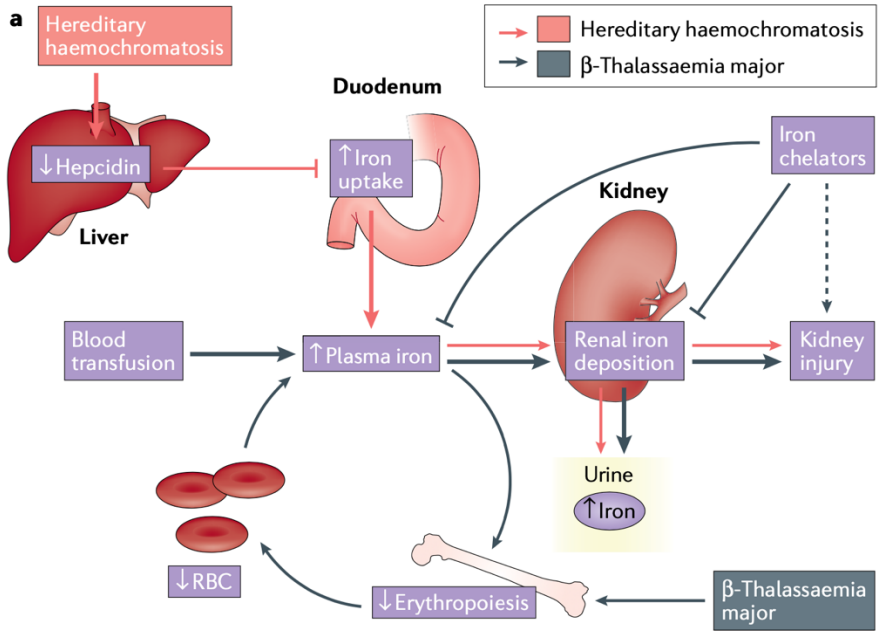

Figure 2-2 Effects of systemic iron overload on kidney. [6]

Meanwhile, kidney dysfunction can also disturb systemic iron homeostasis [6, 41]. Under physiological conditions, iron is filtered by the glomerulus and mostly reabsorbed by the proximal tubule, predominantly in the form of transferrin-binding iron [6]. In renal disease, reduced reabsorption caused by tubular dysfunction or increased leakage caused by glomerulopathy can both lead to increased urinary iron loss [6, 42, 43]. In addition, kidney diseases can also indirectly impact systemic iron availability through inflammation. CKD-induce chronic inflammation impaired iron release from body stores, known as functional iron deficiency (FID) [6]. FID happens through multiple mechanisms; among them, the hepcidin-ferroportin axis is one of the best-known pathway.

doi:10.6342/NTU202210133

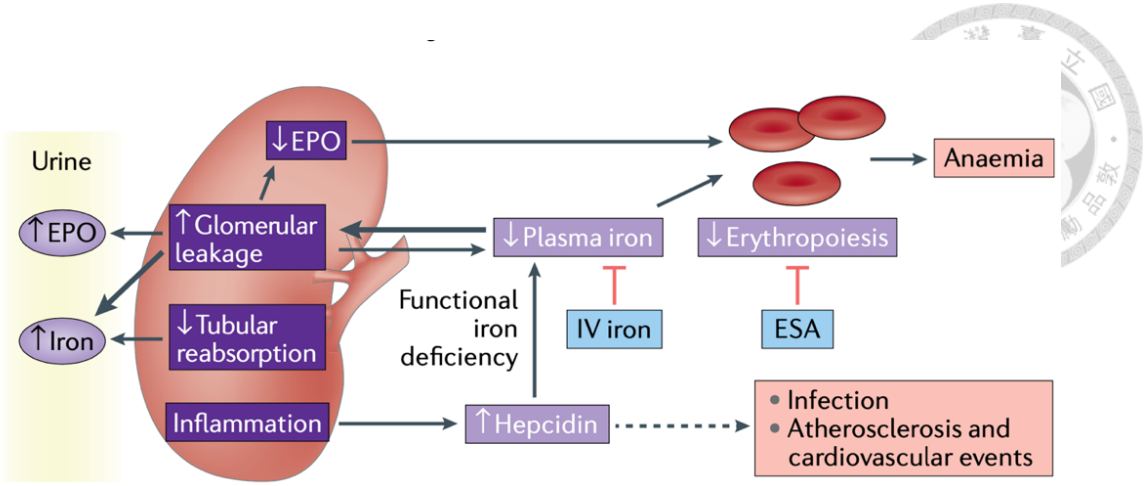

Figure 2-3. Effects of kidney diseases on systemic iron homeostasis [6]

2.1.2 Hemojuvelin and iron regulation

Hepcidin, a 25-amino acid peptide, is a key iron regulator most abundantly expressed by hepatocytes. It downregulates ferroportin, which is the only known iron exporter in mammalian cells. Ferroportin downregulation than decrease iron efflux from cells into the circulation, decreasing systemic iron load [14]. Hepcidin expression is regulated positively by body iron load, mainly through the iron-sensing bone morphogenetic protein 6 (BMP6)- hemojuvelin- bone morphogenetic protein receptor (BMPR) complex [6, 14, 15].

Hemojuvelin (Hjv) is a glycophosphatidylinositol-linked membrane protein, expressed in multiple organs including liver, skeletal muscles, heart, adipocytes, and kidney [10-12]. Together with BMPR, membrane-bond Hjv (mHjv) serves as co-receptor of BMP6. Increased iron storage leads to BMP6 production, which activate the mHjv-BMPR complex. This complex then leads to increased hepcidin transcription, ferroportin degradation, and in the end decrease systemic iron load [6].

In human, failing to express mHjv cause an early-onset form of haemochromatosis called juvenile haemochromatosis [14]. Similarly, knock out of Hjv gene in mice lead to

doi:10.6342/NTU202210133

iron overload and renal iron accumulation [14, 40]. In contrast, excessive mHjv-BMPR complex activation leads to hepcidin overexpression and iron deficiency [44].

The membrane-bound Hjv (mHjv) can be cleaved off by two kinds of enzymes, furin or matriptase-2, and form the soluble Hjv (sHjv) found in serum and urine [11, 14, 16, 17]. Furin cleavage result in 42kDa sHjv in both mice and human [14, 17], while the cleavage pattern of matriptase-2 is currently controversial [45, 46].

While mHjv positively regulate hepcidin, the soluble form (sHjv) exsert an opposite function. This is likely due to its competitive binding to BMP6, decreasing BMP6 binding to the mHjv-BMPR complex [11, 14, 15]. The impact of sHjv on systemic iron regulation is currently unclear, although change of sHjv serum level had been described in several medical conditions, including beta-thalassaemias, anemia of chronic disease, congenital dyserythropoietic anemia type I, anemia during pregnancy, and in patients undergoing haemodialysis [10, 15].

Despite its systemic effect is less well-described, sHjv had been shown to cause local iron deposition in renal tissue. Co-incubation of sHjv with free iron had led to increase iron deposition in human renal cell line (HK2), compared with solely incubated with free iron. Consistently, injection of sHjv aggravate I/R renal injury in mice, as indicated by higher pathological renal injury score. These mice also show significantly increased renal iron deposition, without appreciable changes in liver iron loading [11].

2.1.3 Hemojuvelin in renal diseases

As a close relationship exist between kidney and iron, the role of iron-regulating proteins in renal diseases had attracted research interest. Among them, Hjv had been studied both as a renal injury biomarker and possible therapeutic target.

As above mentioned, serum sHjv had been found to elevated in patients undergoing

doi:10.6342/NTU202210133

hemodialysis [10, 47]. Two studies published on 2012 found sHjv positively related to systemic iron loading markers, such as ferritin and transferrin saturation rate. Meanwhile, it showed no independent correlation with serum hepcidin levels in both studies [10, 47]. In these studies, Hjv was initially considered responding to systemic iron loading, secreted by organs such as liver, skeletal muscle, or heart. However, as Hjv exert its iron-regulating function through hepcidin, the finding that sHjv was not independently related to hepcidin was intriguing. This led to the conclusion that the nature of increased serum sHjv in hemodialysis patients remained to be demonstrated [10].

In 2014, the proteomic study carried out by Yang et al. identified 42kDa sHjv in both human and rats' urine. The urinary sHjv (uHjv) significantly elevated in rats and human with AKI, and Hjv local expression was demonstrated in human's and rats' kidney tissue by IHC [11]. Furthermore, they found that furin inhibitor decreases cleavage of mHjv into sHjv, prevent kidney iron accumulation, reduce renal tubular cell death and protect kidneys from I/R injury both functionally and histologically [11]. In accordance with these finding, Wang et al. [16] and Ko et al. [17] later demonstrated that urinary sHjv, after adjusting with urinary creatinine, predict AKI following cardiac surgery. Urine collected at 3 hours post-surgery was able to independently predict AKI or mortality during hospitalization. The diagnostic ability of creatinine-adjusted hemojuvelin outstands adjusted urinary NGAL, which is a well-known novel AKI biomarker, for advanced AKI and composite outcome [17]. Adding adjusted uHjv, alone [17] or in combination with adjusted urinary kidney injury molecular-1 [16], into established AKI-predicting clinical score also significantly improved score prediction ability.

In 2020, uHjv was successfully demonstrated in feline urine. Different from those found in rats or human urine, Hjv found in feline urine composed of two compartments, weighting 25~35 kDa and 15~25 kDA respectively [18]. The author further demonstrated

doi:10.6342/NTU202210133

that adjusted uHjv, noted as urinary hemojuveline-to-creatinine ratio (UHCR), elevated significantly in cats with kidney disease. There was no significant difference found between CKD, AKI or ACKI groups, while UHCR do increase significantly with more advanced CKD stages [18].

2.2 Lipid oxidation in renal disease

2.2.1 Lipid metabolism in renal disease

CKD is known to disturb lipid homeostasis in both animal model and human, known as CKD-associated dyslipidemia [34, 48-51]. Human with CKD is known to have increased serum cholesterol and triglyceride, with decreased serum high-density lipoprotein (HDL) level [51]. A similar pattern was reported on dogs with CKD [52, 53]. E. Behling-Kelly reported that CKD dogs had a significantly lower serum HDL: non-HDL Ratio, and 55% of dogs with CKD have serum cholesterol level above reference range [53]. Consistently, Brunetto et al. demonstrated that serum low-density/very-low-density lipoprotein (LDL/VLDL) and cholesterol was increased in dogs with CKD [52]. To the best of our knowledge, no similar study had been conducted in cats.

Being a consequence of renal disease, dyslipidemia itself can lead to further renal injury, forming a vicious cycle [48, 49, 53-55]. Hypercholesteremia (> 350 mg/dL) [56] and low HDL [57] had been reported to independently predict renal function decline in general population, as well as in patients with type 2 diabetes mellitus or hypertension [54]. In animal models, dietary with high triglyceride and LDL led to focal segmental glomerulosclerosis, and increased feeding of cholesterol deteriorated proteinuria in puromycin aminonucleoside nephrosis rat model [54]. LDL are known to be pro-inflammatory and lead to lipid accumulation inside vascular wall, both could worsen

doi:10.6342/NTU202210133

kidney injury [48, 54]. Emerging evidences also suggest conformational and functional changes of HDL in CKD. While HDL hold anti-inflammatory and antioxidative effect in healthy individual, it's likely to differ in binding preferences, proteome, and post-translational modification in those with CKD, losing its protective effects and even become harmful [48, 49, 58].

In addition to altered systemic lipid homeostasis, kidney injury also disturbs energy generation from lipid inside renal cells [48, 49]. Kidney overall is highly reliant on lipid as energy source, with different preference between specific cell types; podocytes mainly generate energy through glycolysis, while proximal tubular cells have very limited ability to use glucose and rely heavily on free fatty acids (FFAs) and glutamine. Under normal circumstances, FFAs is uptake by kidney mainly through CD36 receptors. After taken into renal cells, part of FFAs will undergo oxidation inside mitochondria, generating energy, while others stored as complex lipids such as triacylglycerols, diacylglycerols, phospholipids and cholesterol esters [48, 49]. During kidney injury, fatty acid oxidation in renal cells is disrupted, leading to subsequent lack of ATP and lipid accumulation [48, 49, 54, 59].

The significance of impaired fatty acid oxidation in renal disease has been suggested by numerous researches. Fatty acid oxidation had been found to be the most significantly altered metabolism pathway in human with hypertensive or diabetes nephropathy [59]. Down-regulation of fatty acid oxidation lead to renal fibrosis in mice model [59, 60]; meanwhile, enhancing fatty acid oxidation ability protect kidneys from fibrosis and inflammatory changes in a wide range of different kidney injury models, including unilateral ureteral obstruction, folic acid nephropathy, and adenine-induced nephrotoxicity [61].

In veterinary medicine, renal lipid accumulation had been related to cats' renal injury [1,

doi:10.6342/NTU202210133

62-64]. Different from human and dogs, healthy cats can have lipiduria, which is proposed to originate from small lipid droplets inside proximal tubules [65, 66]. However, identifying interstitial free lipid had been reported as a pathologic finding of cats with CKD. In 2015, McLeland et al. carried out a survey on feline CKD pathologic changes. The histologic findings were compared between young control cats, geriatric control cats, and cats with various stages of CKD. They found that interstitial lipid accumulation was noted significantly more frequent in cats with IRIS stage 2~4 CKD; it was noted in 85% of cats with stage 2~4 CKD, compare to 4 out of 21 control cats [63]. Martino-Costa et al. later conducted research that specifically looks into interstitial lipid accumulation in cats and dogs with CKD, which reported interstitial lipid infiltration in 88.9% (24 out of 27) of cats with CKD. Meanwhile, interstitial lipid droplets was not found in any of the 10 control cats, as well as dogs with or without CKD [62]. Additionally, these lipid droplets had been found to consistently associated with inflammatory response, and disorganized/ruptured tubules [1, 62, 64].

2.2.2 Lipid oxidation markers in renal disease

Oxidative stress, defined as imbalance between oxidative and antioxidative system, has long been recognized as a key factor of CKD pathogenesis. Multiple studies have shown increased oxidative stress in CKD patients, and its relation with poor prognosis in this disease [67-69]. Elevated oxidative stress in CKD is multifactorial, resulting from impaired anti-oxidant system, increased reactive oxidative species (ROS) production, and accumulation of a wide variety of other pro-oxidative substances [58, 67, 68, 70, 71]. As above mentioned, altered lipoprotein structure and lipid accumulation had also been recognized as one of oxidative stress sources [49, 54, 70, 72].

As disturbed lipid homeostasis and oxidative stress are both recognized hallmarks of

doi:10.6342/NTU202210133

CKD, lipid oxidation markers had attracted research interest in this field. Malondialdehyde (MDA), one of the best investigated lipid peroxidation product [22], had been used to evaluate lipid oxidation in CKD. Studies in human had found increased plasma MDA in both dialysis and non-dialysis dependent CKD patients, which magnitude correlated with disease severity [25-27].

Beside serum concentration, evaluating oxidative biomarkers in urine has also been proposed a promising method to evaluate oxidative stress in kidney disease. This method holds the advantage that urine has less metal-containing substances, making it theoretically less prone to artificial increase of oxidative stress markers during sample collection and storage [69]. Furthermore, the collection process can be done without invasive manipulation and a sufficient amount of sample can be easily obtained, both makes urinary biomarker an attractive option for veterinary. In patients undergoing liver transplantation, urinary MDA at 2hrs and 24hrs post-surgery was found to significantly predict post-surgery AKI [23]. Also, among critically sick neonates, urinary MDA was significantly higher in those with AKI than those without. Intriguingly, the authors also found that MDA in erythrocytes differed significantly between critically sick and healthy neonates, but not between critically sick neonates with or without AKI. This indicate urinary MDA may be more specific to renal injury, comparing with MDA in systemic circulation [24].

In veterinary medicine, feline with CKD had been reported to have higher serum MDA [28, 29]. Yu and Paetau-Robinson showed a trend toward elevation of serum MDA in cats with CKD, although failed to reach statistical significance ($p = 0.074$), possibly due to small sample size ($n = 10$) or patients being in the relatively early stage (median serum creatinine = 1.9mg/dL) [28]. Valle et al. later reported a statistically significant elevation of serum MDA in cats with IRIS stage 2~4 CKD, and a good correlation of serum MDA

doi:10.6342/NTU202210133

with other serum oxidative stress biomarkers [29].

Regarding urinary oxidative marker in cats, only one study had been published so far to the best of our knowledge. Whitehouse et al. in 2017 looked into F2-isoprostanes concentration in feline urine [73]. They found a significant higher urinary F2-isoprostanes in cats with early-stage CKD (IRIS stage 1~2), compared to cats in more advanced stages. Meanwhile, urinary F2-isoprostanes was significantly lower in cats with advanced stage CKD, compared to that of healthy control. Overall, it showed an elevation of urinary F2-isoprostanes in the early stage of disease, but the concentration decreases as disease further progress [73]. However, the report did not further look into ratio between urinary F2-isoprostanes and creatinine, and the decrease of F2-isoprostanes concentration can possibly be explained by decreased ability to concentrate urine in cats with advanced stage CKD.

2.3 Hemojuvelin and MDA

2.3.1 Impact of lipid dysregulation on iron homeostasis

Lipid accumulation had long been linked to disrupted iron homeostasis, predominantly through inflammation [74-77]. In human, higher body fat links to lower serum total iron across different ages and gender [75]. This can reasonably be explained by the fact that fat tissue secrets a significant amount of pro-inflammatory cytokines, including interleukin-6 (IL-6), tumor necrosis factor alpha (TNF-α), and interleukin-1α [75-77]. This effect can possibly be more prominent in patients with kidney disease, as adipocytes secrets more IL-6 and interleukin-1α under uremic condition [77]. These pro-inflammatory cytokines inhibit iron absorption and release into circulation through multiple pathways, one of which is the up-regulation of hepcidin [14, 75].

doi:10.6342/NTU202210133

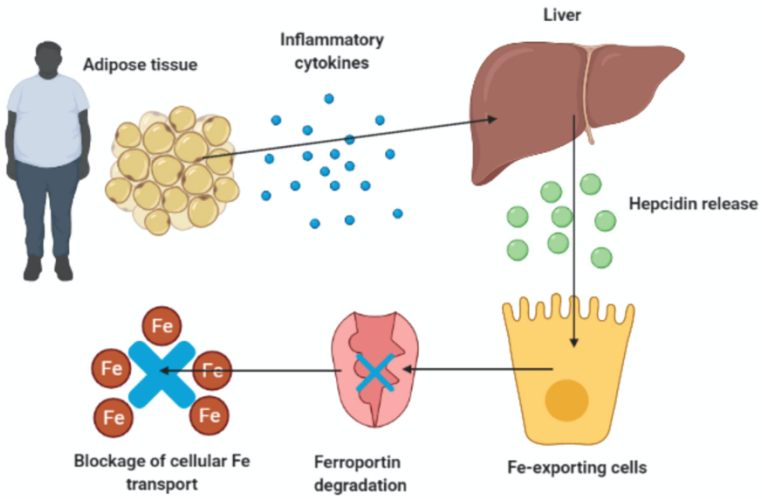

Figure 2-4 Impact of fat tissue to iron availability through hepcidin [75].

As above mentioned, hepcidin regulate systemic iron loading not only through decreasing intestinal iron absorption, but also inhibiting iron exportation from cells into circulation [14]. Therefore, while causing the iron deficiency in the systemic level, it also leads to local iron deposition in the iron-storing organs. This “lipid-hepcidin-iron deposition” axis had been observed in rats’ liver and spleen, where a high-fructose or high-fat diet led to lipid accumulation, pro-inflammatory status, increased hepcidin, and hepatic/splenic local iron accumulation [78, 79]. As renal iron accumulation is also found in renal disease, and serum hepcidin is known to increase in human and feline CKD [80], whether the same mechanism exist in kidneys worth investigation.

In addition to indirect upregulation through inflammation, human and rats’ adipocytes can also directly express hepcidin, and its upstream regulator Hjv [12]. The expression of hepcidin is significantly correlated mHjv, and can be positively regulated via BMP-Hjv pathway in vitro, implying adipocyte local-expressed hepcidin is at least partly regulated by its expression of mHjv [12]. Whether this local expression of Hjv and hepcidin plays significant role in iron status is yet to be determined.

doi:10.6342/NTU202210133

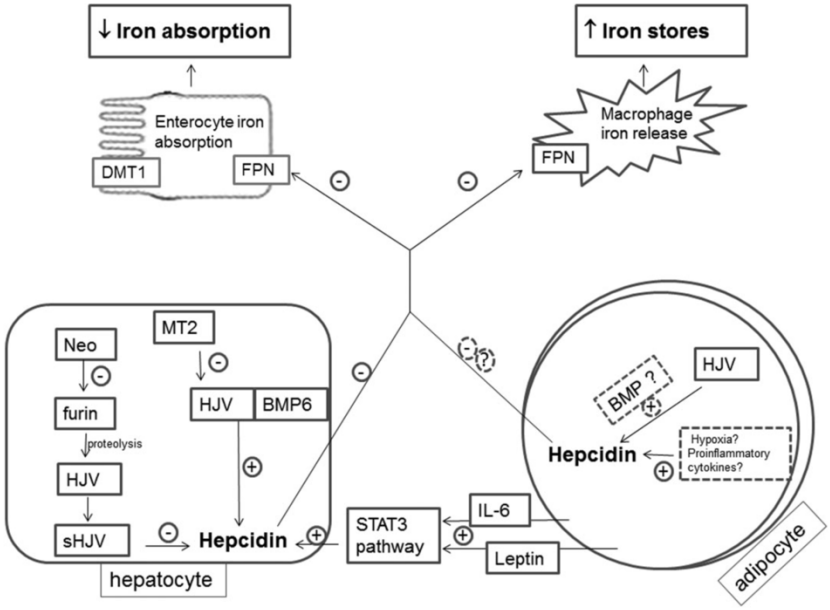

Figure 2-5 The relationship between iron and hepcidin in adipocyte and hepatocyte [81].

2.3.2 Role of iron in lipid oxidation

As above mentioned, iron has been known as a source of oxidative stress in kidney diseases. This iron-origin oxidative stress targets a wide range of substances including DNA, protein, and lipid; among them, the effect it has on lipid had attracted research interest regarding its unique mechanism and consequences.

Iron is a critical catalyzer in the lipid peroxidation process, which is the process leading to production of lipid oxidative stress markers ex. MDA [82]. During peroxidation, lipid first loss one hydrogen atom, become a lipid radical; then react with diatomic oxygen and abstract hydrogen atom from other lipid species, forming lipid peroxides (L–OOH). This lipid peroxides can then be catalyzed by transition metals— most often, iron— then become a lipid alkoxyl radicals that is also highly reactive, attacking other lipid species, contribute to the vicious cycle [82]. The dependency of lipid peroxidation to iron has been proved in various kinds of models, showing that iron chelator can fully suppress lipid

doi:10.6342/NTU202210133

peroxidation induced by disrupted intracellular antioxidant system [82].

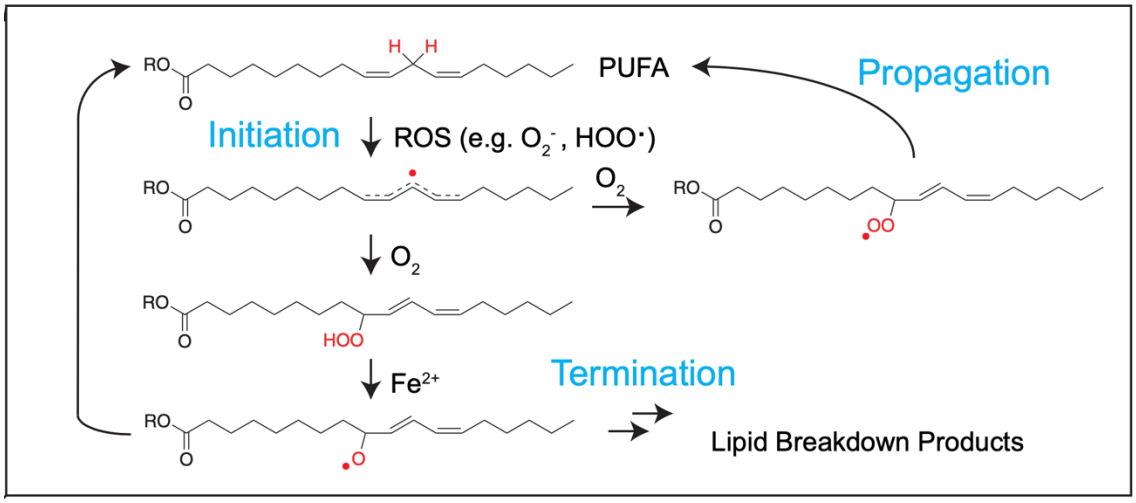

Figure 2-6 Lipid peroxidation process. [82]

The significance of iron-origin lipid peroxidation had also been found in renal disease. Reduce iron intake led to lower renal tissue MDA in diabetic nephropathy model, along with decreased albuminuria and histologic lesion [8]. AKI induced by myoglobulin was found related to lipid peroxidation inside renal tubular cells, likely induced by iron inside myoglobulin [83, 84].

Another clear demonstration of iron-related lipid oxidation stress is ferroptosis. As above mentioned, ferroptosis had been reported closely related to kidney diseases. Recently, the relation between free iron, ferroptosis, and feline kidney disease was explored (Huang et al. 2022, unpublished data). Huang et al. found that serum free iron, after correcting with hematocrit, and urinary GPX4, after correcting with urinary creatinine, elevated significantly along with the decline of renal function. Additionally, these two markers both significantly predict feline CKD progression within 90 days, and correlated positively with each other. This indicates a possible role of iron-originated injury and lipid oxidation in feline CKD, and warrant a further exploration into the underlying mechanism behind the disrupted iron homeostasis.

doi:10.6342/NTU202210133

2.3.3 Hemojuvelin and lipid oxidative stress

As above mentioned, hepcidin has been found to play a role in interaction between iron and lipid metabolism, being induced or directly secreted by adipocytes than impact iron homeostasis. On the other hand, hepcidin can regulate lipid oxidative stress, possibly through the hemojuvelin-hepcidin-ferroportin pathway.

Hepcidin had been found to be up-regulated in cardiomyocytes undergoing ischemia-reperfusion injury, possibly induced by increased iron loading [85]. This up-regulation is proposed to be a protective mechanism, preventing iron release from macrophage thus protect cells from iron-origin oxidative stress. This proposed protective effect was later supported by Bayraktar et al. finding. They showed that treatment with hepcidin significantly reduced MDA level in rats' heart undergoing ischemia-reperfusion treatment [19]. The similar finding of hepcidin protect against lipid oxidation was also reported in colorectal cancer epithelial cells [20].

As mHjv serve as the main pathway of iron-responsive hepcidin up-regulation, it is reasonable to suggest mHjv participate in this hepcidin protective function against iron-overload and lipid oxidation. This hypothesis also fits the above-mentioned findings in rats' kidneys; mHjv cleavage was followed by profound renal iron deposition, and inhibiting mHjv cleavage can significantly ameliorate iron deposition and the following renal injury [11]. Folgueras et al. had also showed that Matriptase-2 deficiency leads to improved lipid metabolism, and this effect can be fully reverted by anti-Hjv antibody [21]. This suggested a role of Hjv in regulating proper lipid metabolism, thus protecting cells from lipid oxidation stress.

doi:10.6342/NTU202210133

Chapter 3 Materials and Methods

3.1 Patients and sample collection

3.1.1 Case selection and follow-up

Cats conducted urinary analysis in National Taiwan University Veterinary Hospital (NTUVH) (Taipei, Taiwan) over January 2018 to November 2021 were surveyed. Cats that meet one or more of the following criteria were retrospectively enrolled in the CKD group: (1) Plasma creatinine ≥ 1.6 mg/dL; (2) Inadequate urinary concentrating ability (e.g. urine specific gravity < 1.030); (3) Abnormal renal imaging findings under ultrasonography or radiography exam.

The above-mentioned findings should persist for > 30days, and without any identifiable non-renal causes. Cases will be excluded if presented with malignancy, liver abnormalities (ex. elevated liver indexes), suspected systemic infectious/inflammatory status (ex. FIV, FeLV, leukocytosis), or abnormal thyroid function (ex. hyperthyroidism).

The remaining cases will then be classified according to IRIS staging of CKD (2019). Meanwhile, cases with sufficient follow-up data will also be classified into progression or non-progression group. Progression is defined as creatinine increase ≥ 0.5 mg/dL.

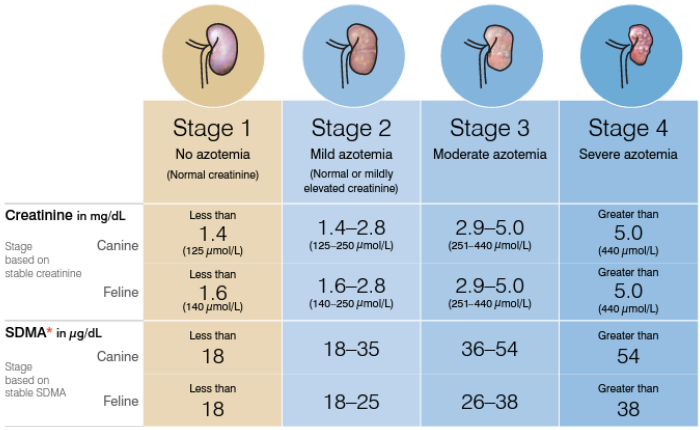

		Stage 1 No azotemia (Normal creatinine)	Stage 2 Mild azotemia (Normal or mildly elevated creatinine)	Stage 3 Moderate azotemia	Stage 4 Severe azotemia
Creatinine in mg/dL					
Stage based on stable creatinine	Canine	Less than 1.4 (125 µmol/L)	1.4–2.8 (125–250 µmol/L)	2.9–5.0 (251–440 µmol/L)	Greater than 5.0 (440 µmol/L)
	Feline	Less than 1.6 (140 µmol/L)	1.6–2.8 (140–250 µmol/L)	2.9–5.0 (251–440 µmol/L)	Greater than 5.0 (440 µmol/L)
SDMA* in µg/dL					
Stage based on stable SDMA	Canine	Less than 18	18–35	36–54	Greater than 54
	Feline	Less than 18	18–25	26–38	Greater than 38

Figure 3-1 IRIS staging system for canine and feline CKD.

doi:10.6342/NTU202210133

3.1.2 Sample collection and storage

Urine samples obtained for diagnosis purpose in NTUVH were collected. Urine was centrifuged, and supernatant were stored at -80°C refrigerator.

3.1.3 Clinical parameters measurements

For the included cases, the medical history, physical exam, blood exam, urinary analysis, and other relevant exams results were retrieved. Hematologic values were measured by Exigo hematology analyzer. Plasma chemistry values were measured by Ortho Clinical DiagnosicsTM VITROSTM350 system; the globulin concentration was calculated as total protein minus albumin. Plasma electrolytes were measured by Roche Cobas b 121 system. Urine analysis were conducted using Roche Cobas b 411 system.

3.2 Urinary MDA measurement

Protocol of feline urinary MDA measurement had been previously established and used here (Chang et al. 2021, unpublished data). In brief, Urinary MDA was measured as thiobarbituric acid reactive substances (TBARS) as previously described [86]. Thiobarbituric acid and MDA forms MDA-TBA_2 complex, which is chemically stable and holds a distinct pink color. The MDA-TBA_2 complex concentration was than measured by high performance liquid chromatography (HPLC), therefore determine MDA concentration.

doi:10.6342/NTU202210133

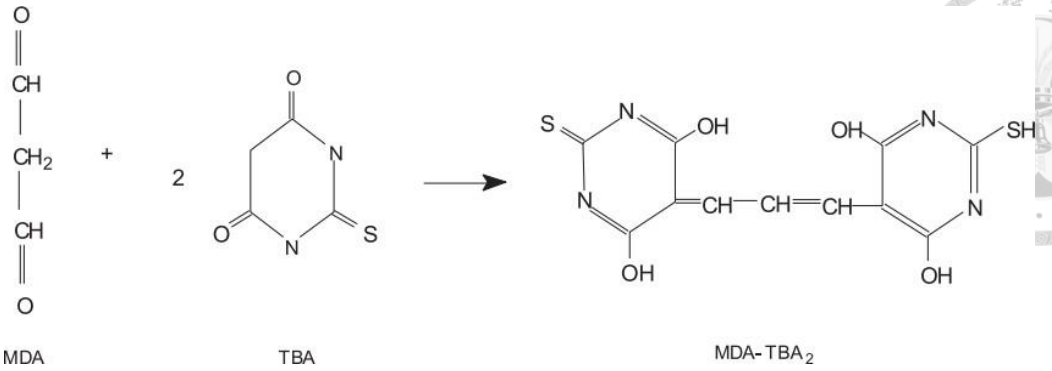

Figure 3-2 Thiobarbituric acid (TBA) and MDA forms MDA-TBA_2 complex [86].

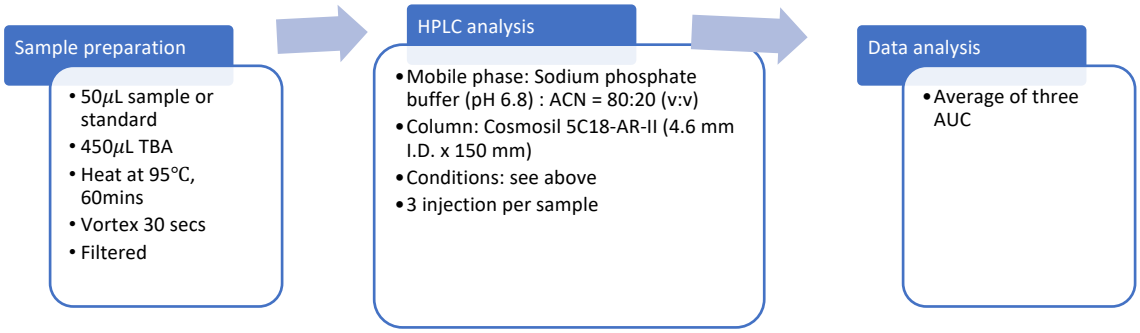

Figure 3-3 Flow chart of urinary MDA analysis by HPLC.

3.2.1 Chemicals and reagents

1. 1,1,3,3-Tetramethoxypropane , 99% (Merck KGaA, Germany)
2. Acetonitrile (ACN), ≥ 99.9% (J.T. Baker, Holland)
3. 2-Thiobarbituric acid (TBA), ≥ 98% ((Merck KGaA, Germany)
4. Sodium hydrogen phosphate, 99% (PANREAC chemicals, Spain)
5. Sodium phosphate monobasic, ≥ 99.9% (Sigma-Aldrich, USA)

3.2.2 Supplies

1. Blood collection syringe: 1 ml syringe (Terumo, Belgium)
2. Syringe filter, PTFE, 13 mm, 0.45 μm (MyTech, Taiwan)

doi:10.6342/NTU202210133

3.2.3 Apparatus

1. pH meter: SP-2300 (Suntex, Taiwan)
2. Genius dry bath incubator, MD-02N (Major science, USA)
3. Agilent 1260 Infinity II (Agilent Technologies, USA)
4. HPLC column: Cosmosil 5C18-AR-II column (4.6 mm I.D. x 150 mm)

3.2.4 HPLC conditions

The HPLC protocol was modified from previous research [87].

1. Mobile phase: Sodium phosphate buffer (pH 6.8)-Acetonitrile (80:20, v/v), preparation protocol was listed as follow:

1.1. Dissolve sodium hydrogen phosphate 0.9 g and sodium phosphate monobasic 1.6 g into 1000 ml of double distilled water to make 20 mM, pH 6.7 sodium phosphate buffer.

1.2. Mix sodium phosphate buffer solution with acetonitrile in 80:20 (v/v).

2. Flow rate: 1.3 ml/min
3. Excitation wavelength: 532 nm
4. Emission wavelength: 553 nm
5. Injection volume: 50 μL

3.2.5 Sample and standard solution preparation

Urine was stored at -80°C and unfreeze at room temperature before processing. Standard solutions were prepared from 1,1,3,3-Tetramethoxypropane, diluting into 4000, 1000, 250, 62.5 ppb. All samples and standards were measured in triplicate, and concentrations determined by averaging three levels.

Sample and standards will then be processed with the following protocol:

doi:10.6342/NTU202210133

1. Preparing 25 mM, pH 3.5 TBA solution (TBA 0.18 g, sodium phosphate monobasic 1.692 g and phosphoric acid 40 μL dissolved into 50 ml of double distilled water)
2. Mix 50 μL urine with 450 μL TBA solution. Vortex the mixture, then incubate at 95°C for 60 minutes.
3. Cool the samples in ice bath for 5 minutes, then adapt samples to room temperature.
4. Vortex samples, then filtered with syringe PTFE filter (13 mm, 0.45 μm).
5. HPLC analysis were conducted under above-mentioned condition.

3.3 Urinary Hjv measurement

Urine was stored at -80°C and unfreeze at room temperature before processing. Urinary Hjv was measured using commercial quantitative sandwich ELISA Kit designed for feline hemojuvelin quantification (Catalog# MBS1608274, Mybiosource, USA). Measurement was conducted following protocol provided by manufacturer.

All samples and standards were measured in duplicate, and concentrations determined by averaging two levels. Standards were prepared to a final concentration of 32, 16, 8, 4, 2 ng/ml, as manufacturer instruction. The assay protocol listed below:

1. All reagents and samples brought to room temperature and allowed fully unfreeze.
2. Add 50μl of standard into each standard well.
3. Add 40μl sample to sample wells and then add 10μl anti-HJV antibody to sample wells, then add 50μl streptavidin-HRP to sample wells and standard wells.
4. Mix well. Cover the plate with a sealer. Incubate 60 minutes at 37°C.
5. Remove the sealer and wash the plate 5 times with wash buffer. Soak wells with 300ul wash buffer for 30 seconds to 1 minute for each wash.

doi:10.6342/NTU202210133

6. Add 50μl substrate solution A to each well and then add 50μl substrate solution B to each well.
7. Incubate plate covered with a new sealer for 10 minutes at 37°C in the dark.
8. Add 50μl Stop Solution to each well.
9. Determine the optical density (OD value) of each well immediately using a microplate reader set to 450 nm.

3.4 Statistical analysis

SPSS software package (v.26) was used for the statistical analysis.

Clinical parameters between groups were compared using Mann–Whitney U test (continuous) or Chi-square (categorical).

Linear correlation between continuous parameters were evaluated via linear regression models. All parameters will first be analyzed with simple linear regression model. Parameters with p-value < 0.1 will then be enrolled into forward stepwise multiple linear regression, with criteria of $p < 0.05$ as enter, $p > 0.10$ as remove.

The prediction value of parameters to 90-day progression were evaluated through logistic regression. The prediction value of parameter of interest (urinary Hjv and MDA) were further evaluated through Receiver operating characteristic (ROC) curve, Kaplan-Meier curves, and Cox proportional hazards regression; simple and multiple Cox proportional hazard regression will be conduct with the same manner as linear regression analysis (all parameters first analyzed with simple Cox regression model; parameters with p-value < 0.1 will then be enrolled into forward stepwise multiple Cox regression, with criteria of $p < 0.05$ as enter, $p > 0.10$ as remove).

Significance was defined as p-value less than 0.05.

doi:10.6342/NTU202210133

Chapter 4 Results

4.1 Feline urinary Hjv and MDA measurement

4.1.1 Feline urinary MDA measurement

MDA standard curve was established at concentration of 4000, 1000, 250, 62.5 ppb. The coefficient of determination for the standard curve was 0.9971. The inter-CV was 2.712% for 4000ppb, 3.398% for 1000ppb, 3.685% for 250ppb, and 6.034 for 62.5ppb. The intra-CV was 4.375% for 4000ppb, 0.848% for 1000ppb, 1.382% for 250ppb, and 2.192% for 62.5ppb (Table 4-1, Figure 4-1). The median retention time was 2.29 minutes, with standard deviation of 0.026mins.

Table 4-1 Details of MDA standard curve establishment.

Validation details	
Calibration curve	AUC = 0.0803*concentration (ppb) + 14.133. R^2 = 0.9971.
Inter-assays CV	2.712% (4000ppb), 3.398% (1000ppb), 3.685% (250ppb), 6.034% (62.5ppb)
Intra-assays CV	4.375% (4000ppb), 0.848% (1000ppb), 1.382% (250ppb), 2.192% (62.5ppb)

Abbreviation: CV, Coefficients of Variability; AUC, area under curve

doi:10.6342/NTU202210133

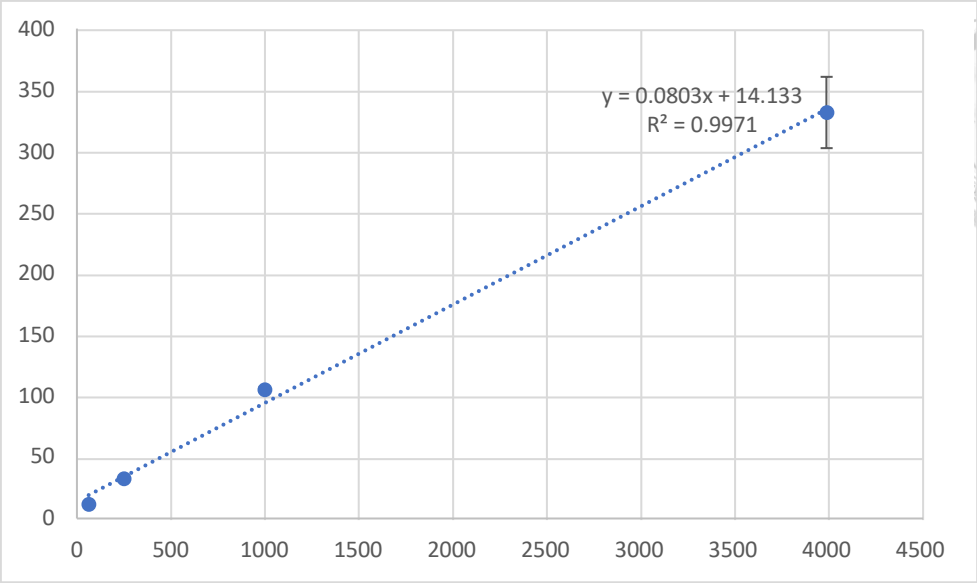

Figure 4-1 MDA standard curve.

Error bar: 1.96* Standard deviation.

Standard curve was established at concentration of 4000, 1000, 250, 62.5 ppb. The linear regression equation is AUC = 0.0803*concentration (ppb) + 14.133 and R square = 0.9971.

4.1.2 Feline urinary Hjv measurement

Feline urinary Hjv were measured using commercial kit as above mentioned. Standard curves were established with concentration of 32, 16, 8, 4, 2 ng/ml following manufacturers' instruction. the coefficient of determination for the standard curve was 0.9966 (Figure 4-2). The inter-CV was less than 10%, and intra-CV was less than 8% following manufacturer's instruction.

doi:10.6342/NTU202210133

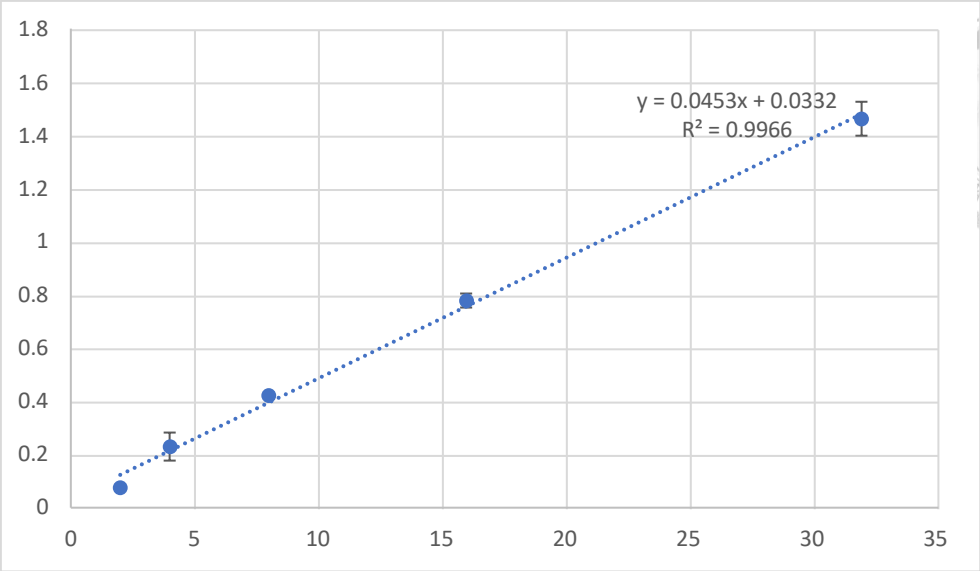

Figure 4-2 Hjv standard curve.

Standard curve was established at concentration of 32, 16, 8, 4, 2 ng/ml. The linear regression equation is O.D. (450nm) = 0.0453*concentration (ng/ml) +0.0332, R square = 0.9966.

4.2 Urinary Hjv and MDA in CKD cats

4.2.1 Cases population

A total of 60 cats fit the above-mentioned criteria and were included in the study. This included 35 domestic short hair; 4 American short hair; 4 Persian and 1 Persian mix; 4 Chinchilla; 3 Scottish fold; 3 English short hair; 2 Bengal; 2 domestic long hair; 1 exotic long hair; and 1 Russian blue.

According to IRIS CKD staging system, there were 2 cats in stage 1, both included due to persistent hyposthenuria (USG < 1.030 for more than 2 occasions 30 days apart). 39 cats were in stage 2, 15 cats in stage 3, and 4 cats in stage 4 CKD. As the case number for CKD stage 1 (n = 2) and stage 4 (n = 4) was small, cats were alternatively grouped into early-stage (stage 1 and 2) and late-stage (stage 3 and 4) CKD.

doi:10.6342/NTU202210133

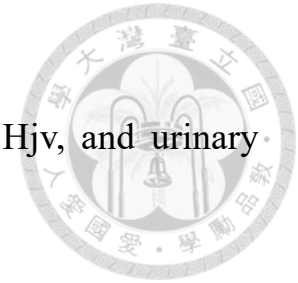

4.2.2 Correlation between clinical parameters, urinary Hjv, and urinary MDA in CKD cats

The clinical parameters, urinary Hjv, and urinary MDA of cats are summed up in Table 4-2. Among 60 cases included in the study, 7 cases' urinary Hjv were lower than detection limits, and were counted as zero for statistics purpose.

Cats with late-stage CKD was significantly older, with no significant different in sex distribution. Also, cats with late-stage CKD had significantly lower hematocrit and Urinary-specific gravity (USG), and significantly higher serum potassium, urinary protein-to-creatinine ratio (UPC), and blood urea nitrate (BUN) (Table 4-2).

To account for decreased urinary concentration ability in cats with kidney disease, the urinary Hjv and MDA was adjusted with urinary creatinine, as previous researches in human and cats [4, 16-18]. Adjusted Hjv and MDA was noted as urinary Hjv-to-creatinine ratio (UHCR) and urinary MDA-to-creatinine (UMCR), respectively. In accordance with previous researches, UHCR was significantly higher in cats with advances CKD, in comparison with those with early-stage CKD (median [IQR], 52.58 [10.69, 92.70] $*10^{-7}$ in late-stage vs. 15.47 [4.88, 47.74] $*10^{-7}$ in early-stage; p-value, 0.032). On the other hand, UMCR showed no significant difference between early- and late-stage (median [IQR], 5.46 [3.71, 10.26] ppb/mg/dL in early-stage vs. 6.65 [4.30, 11.01] ppb/mg/dL in late-stage; p-value, 0.395). Urinary Hjv had no significant difference between groups (median [IQR], 2.98 [1.43, 4.40] ng/mL in early stage vs. 3.90 [2.04, 5.69] ng/mL in late-stage; p-value, 0.106), and urinary MDA was significantly higher in cats with early-stage CKD than those with late-stage CKD (median [IQR], 962.16 [551.63, 1736.40] ppb in early-stage vs. 528.48 [301.98, 1084.88] ppb in late-stage; p-value, 0.038). Other clinical

doi:10.6342/NTU202210133

parameters showed a significant difference between early- and late- stage CKD included: uCrea, age, sCrea, hematocrit, BUN, potassium, USG, and UPC (Table 4-2).

Table 4-2 The clinical parameters, urinary Hjv, and urinary MDA of CKD cats.

Parameters	Early stage (n = 41)		Late stage (n = 19)		P value
uCrea (mg/dL)	185.8 (88.1, 256.05)	N = 41	74.4 (49.3, 137.2)	N = 19	0.003*
uHjv (ng/mL)	2.98 (1.43, 4.40)	N = 41	3.90 (2.04, 5.69)	N = 19	0.106
UHCR (*10^{-7})	15.47 (4.88, 47.74)	N = 41	52.58 (10.69, 92.70)	N = 19	0.032*
uMDA (ppb)	962.16 (551.63, 1736.40)	N = 41	528.48 (301.98, 1084.88)	N = 19	0.038*
UMCR (ppb/mg/dL)	5.46 (3.71, 10.26)	N = 41	6.65 (4.30, 11.01)	N = 19	0.395
Age (years)	6 (4, 11.5)	N = 41	14 (9, 15)	N = 19	0.002*
Sex (%Female)	56.1%	N = 41	36.8%	N = 41	0.267
BW (kg)	4.55 (3.635, 5.18)	N = 38	3.96 (3.00, 5.14)	N = 19	0.157
sCrea (mg/dL)	2.2 (1.85, 2.3)	N = 41	3.7 (3.2, 4.7)	N = 19	< 0.001**
Sys BP (mmHg)	158.5 (135.75, 181.00)	N = 8	146 (137.5, 159.5)	N = 13	0.456
Hct (%)	40.3 (33.3, 44.3)	N = 33	28.9 (27.35, 35.80)	N = 17	0.003*
WBC ($10^3/\mu$L)	7400 (5850, 9500)	N = 33	7700 (6150, 9950)	N = 17	0.712
Albumin (g/dL)	3.300 (3.175, 3.500)	N = 30	3.3 (3.2, 3.6)	N = 15	0.645
Globulin (g/dL)	4.2 (3.9, 4.5)	N = 19	4.25 (3.75, 4.675)	N = 8	0.856
A/G ratio	0.81 (0.73, 0.88)	N = 19	0.83 (0.79, 0.9475)	N = 8	0.515
Glucose (mg/dL)	113.50 (93.75, 137.50)	N = 22	120 (98.5, 142)	N = 9	0.507
BUN (mg/dL)	27 (22, 31)	N = 41	50 (39, 74)	N = 19	< 0.001**
Phosphorus (mg/dL)	4.3 (3.6, 5.2)	N = 27	4.7 (3.6, 6.85)	N = 17	0.173
Sodium (mmol/L)	155.25 (152.85, 157.43)	N = 34	155 (152.18, 157.93)	N = 18	0.908
Potassium (mmol/L)	3.805 (3.525, 4.1225)	N = 34	4.27 (3.725, 4.6275)	N = 18	0.018*
Chloride (mmol/L)	117.95 (116.45, 119.15)	N = 34	118.1 (116.15, 119.875)	N = 18	0.946
ALKP (U/L)	38 (31, 50)	N = 15	36 (31.5, 39)	N = 5	0.553
ALT (U/L)	45 (36, 67)	N = 17	52 (45.5, 99)	N = 5	0.164
AST (U/L)	28 (21, 33)	N = 15	26 (24.5, 34,5)	N = 5	0.866
USG	1.018 (1.013, 1.030)	N = 41	1.011 (1.009, 1.013)	N = 19	< 0.001**
UPC	0.075 (0.04, 0.23)	N = 20	0.45 (0.2625, 1.2325)	N = 10	0.005*

Data are presented as median (IQR). Difference between groups were evaluated using Mann–Whitney U test (continuous) or Chi-square (categorical).

* Indicates $p < 0.05$. ** indicates $p < 0.001$.

Abbreviation: uCrea, urinary creatinine; uHjv, urinary hemojuvelin; UHCR, urinary hemojuvelin-to-creatinine ratio; uMDA, urinary malondialdehyde; UMCR, urine malondialdehyde-to-creatinine ratio; BW, body weight; sCrea, serum creatinine; Sys BP, systolic arterial pressure; Hct, hematocrit; WBC, white blood cell count; A/G ratio, serum albumin-to-globulin ratio; BUN, blood urea nitrogen; ALKP, alkaline phosphatase; ALT, alanine aminotransferase; AST, aspartate aminotransferase; USG, urinary specific gravity; UPC, urine protein-to-creatinine ratio.

doi:10.6342/NTU202210133

The relation between UHCR, UMCR and other clinical parameters were explored using linear regression analysis and summed in Table 4-3. All parameters' relation with UHCR or UMCR were first surveyed using simple linear regression analysis. Those parameters with p value < 0.1 were further included into forward stepwise multiple linear regression analysis, except that uMDA were not included into UHCR linear regression model due to its dependency with UMCR.

For UHCR linear regression model, simple linear regression analysis revealed a significant positive correlation with UMCR, globulin and BUN; and a significant negative correlation with uMDA and USG. In addition to above-mentioned parameters, Hct, sodium, UPC and BW also hold p value less than 0.1 and were enrolled into multiple linear regression analysis. When stepwise multiple linear regression applied, only BUN and USG remained in the model, with p-value of 0.001 and 0.009, respectively (Table 4-3).

As for UMCR, simple linear regression analysis showed significant positive UHCR, BUN, potassium, and age. UHCR, A/G ratio, BUN, potassium and age were enrolled into stepwise multiple linear regression analysis, and only potassium remained in the model with p-value of 0.007 (Table 4-3).

doi:10.6342/NTU202210133

Table 4-3 Simple and stepwise multiple linear regression analysis of UHCR/UMCR, and other clinical parameters.

	UHCR						UMCR					
	Simple linear regression			Stepwise multiple linear regression			Simple linear regression			Stepwise multiple linear regression		
Parameters	Adjusted β	t-value	p-value	Adjusted β	t-value	p-value	Adjusted β	t-value	p-value	Adjusted β	t-value	p-value
uHjv	-	-	-				0.198	1.541	0.129			
UHCR	-	-	-				0.342	2.775	**0.007***			
uMDA	-0.372	-3.054	0.003*				-	-	-			
UMCR	0.342	2.775	**0.007***				-	-	-			
sCrea (mg/dL)	0.177	1.373	0.175				0.186	1.441	0.155			
Sys BP (mmHg)	0.099	0.435	0.668				0.278	1.260	0.223			
Hct (%)	-0.292	-2.113	**0.040***				-0.163	-1.147	0.257			
WBC ($10^3/\mu$L)	0.155	1.084	0.284				-0.016	-0.113	0.910			
Alb (g/dL)	-0.053	-0.350	0.728				0.160	1.062	0.294			
Globulin (g/dL)	0.450	2.520	**0.018***				-0.280	-1.457	0.157			
A/G ratio	-0.231	-1.190	0.245				0.332	1.759	**0.091**			
Glucose (mg/dL)	0.006	0.031	0.976				0.169	0.923	0.364			
BUN (mg/dL)	0.349	2.835	**0.006***	0.631	4.619	0.001*	0.285	2.262	**0.027***			
Phos (mg/dL)	0.126	0.823	0.415				-0.019	-0.125	0.901			
Sodium (mmol/L)	-0.236	-1.719	**0.092**				0.108	0.770	0.445			
Potassium (mmol/L)	0.135	0.961	0.341				0.291	2.148	**0.037***	0.518	2.963	0.007*
Chloride (mmol/L)	-0.159	-1.139	0.260				0.171	1.229	0.225			
ALKP (U/L)	-0.306	-1.362	0.190				-0.131	-0.559	0.583			
ALT (U/L)	-0.044	-0.196	0.847				0.051	0.230	0.821			
AST (U/L)	-0.075	-0.320	0.752				0.283	1.250	0.227			
USG	-0.481	-4.177	**< 0.001****	-0.450	-3.298	0.009*	-0.145	-1.120	0.267			
UPC	0.314	1.749	**0.091**				0.188	1.015	0.319			
Age (years)	0.140	1.076	0.287				0.292	2.322	**0.024***			
BW (kg)	-0.256	-1.965	**0.054**				0.051	0.381	0.705			

doi:10.6342/NTU202210133

* Indicates $p < 0.05$. ** indicates $p < 0.001$. Bold font indicates $p < 0.1$ and enrollment into multiple linear regression.

Abbreviation: uHjv, urinary hemojuvelin; UHCR, urinary hemojuvelin-to-creatinine ratio; uMDA, urinary malondialdehyde; UMCR, urine malondialdehyde-to-creatinine ratio; BW, body weight; sCrea, serum creatinine; Sys BP, systolic arterial pressure; Hct, hematocrit; WBC, white blood cell count; A/G ratio, serum albumin-to-globulin ratio; BUN, blood urea nitrogen; ALKP, alkaline phosphatase; ALT, alanine aminotransferase; AST, aspartate aminotransferase; USG, urinary specific gravity; UPC, urine protein-to-creatinine ratio.

doi:10.6342/NTU202210133

To verify the nature of correlation between UHCR and UMCR, the regression model was separately corrected with Hct, globulin, BUN, USG and BW, with UHCR as dependent variable (Table 4-4). Also, the regression model was separately corrected with BUN, potassium, and age with UMCR as dependent variable (Table 4-5). The result showed that correlation between UHCR and UMCR is independent of all above parameters, except that UMCR concurrent change with UHCR will be explained by concurrent change of globulin.

Table 4-4 Linear regression model of UMCR correlation with UHCR. UHCR was set as the dependent variable, and UMCR parameter in the models was shown.

Adjustment Model	**UMCR Standardized B**	**t**	**p**
(non)	0.342	2.775	0.007*
Model A	0.320	2.549	0.014*
Model B	0.310	2.315	0.025*
Model C	0.166	0.891	0.382
Model D	0.264	2.121	0.038*
Model E	0.374	2.902	0.006*
Model F	0.278	2.497	0.015*
Model G	0.360	2.946	0.005*

* Indicates $p < 0.05$.

Model A = adjusted with sCrea; Model B = adjusted with Hct; Model C = adjusted with globulin; Model D = adjusted with BUN; Model E = adjusted with sodium; Model F = adjusted with USG; Model G = adjusted with BW.

Abbreviation: UHCR, urinary hemojuvelin-to-creatinine ratio; UMCR, urine malondialdehyde-to-creatinine ratio; BW, body weight; sCrea, serum creatinine; Hct, hematocrit; BUN, blood urea nitrogen; USG, urinary specific gravity.

doi:10.6342/NTU202210133

Table 4-5 Linear regression model of UMCR correlation with UHCR. UMCR was set as the dependent variable, and UHCR parameter in the models was shown.

Adjustment Model	UHCR Standardized B	t	p
(non)	0.342	2.775	0.007*
Model A	0.319	2.549	0.014*
Model B	0.277	2.121	0.038*
Model C	0.311	2.380	0.021*
Model D	0.308	2.536	0.014*

* Indicates $p < 0.05$.

Model A = adjusted with sCrea; Model B = adjusted with BUN; Model C = adjusted with Potassium; Model D = adjusted with age.

Abbreviation: UHCR, urinary hemojuvelin-to-creatinine ratio; UMCR, urine malondialdehyde-to-creatinine ratio; sCrea, serum creatinine; BUN, blood urea nitrogen.

4.3 Correlation between UHCR, UMCR, and feline CKD progression

4.3.1 Correlation of clinical parameters, UHCR, UMCR, and progression within 90 days

Characteristics were compared between cats who have their CKD progressed (creatinine elevation ≥ 0.5 mg/dL) within 90 days and those who have not. 18 cats were included into progressed group, while 30 cats were included into non-progressed group.

The uHjv, uMDA, UHCR, UMCR and other clinical parameters were compared between progressed and non-progressed group and shown in Table 4-6. UHCR, age, sCrea, BUN and potassium were significantly higher in cats with progressed CKD, while uMDA, Hct and USG was significantly lower.

doi:10.6342/NTU202210133

Table 4-6 Characteristics of cats progressed within 90 days and those did not.

	Non-progressed (n = 30)		Progressed (n = 18)		P value
uHjv (ng/mL)	2.94 (1.48, 4.78)	N = 30	3.65 (2.01, 6.01)	N = 18	0.277
UHCR (*10^{-7})	15.89 (5.58, 39.55)	N = 30	54.42 (25.31, 97.96)	N = 18	0.009*
uMDA (ppb)	1095.75 (541.00, 2057.35)	N = 30	505.82 (295.37, 754.56)	N = 18	0.003*
UMCR (ppb/mg/dL)	5.889 (3.906, 8.652)	N = 30	5.583 (3.821, 16.851)	N = 18	0.701
Age (years)	6 (4, 11.25)	N = 30	14 (8.5, 16)	N = 18	0.002*
Sex (%F)	53.3%	N = 30	50.0%	N = 18	0.823
BW (kg)	4.45 (3.56, 4.96)	N = 27	4.12 (2.98, 5.26)	N = 18	0.366
sCrea (mg/dL)	2.2 (1.9, 2.5)	N = 30	3.35 (2.375, 4.3)	N = 18	< 0.001**
Sys BP (mmHg)	159.0 (133.75, 186.25)	N = 6	147.5 (138.75, 159.5)	N = 10	0.562
Hct (%)	40.45 (32.55, 44.13)	N = 26	31.7 (27.83, 35.88)	N = 16	0.008*
WBC ($10^3/\mu$L)	7000 (5550, 8900)	N = 26	8100 (6675, 10675)	N = 16	0.162
Alb (g/dL)	3.3 (3.2, 3.5)	N = 24	3.3 (3.1, 3.5)	N = 15	0.700
Globulin (g/dL)	4.2 (3.93, 4.45)	N = 16	4.3 (3.9, 4.8)	N = 7	0.579
A/G ratio	0.81 (0.73, 0.87)	N = 16	0.81 (0.79, 0.88)	N = 7	0.871
Glucose (mg/dL)	113.5 (94.75, 137.5)	N = 18	121.5 (92.75, 145.5)	N = 8	0.765
BUN (mg/dL)	27.5 (22.0, 31.0)	N = 30	49.5 (34.0, 72.5)	N = 18	< 0.001**
Phosphorus (mg/dL)	4.4 (4.0, 5.4)	N = 21	4.7 (3.1, 6.3)	N = 15	0.34
Sodium (mmol/L)	155.8 (153.4, 157.9)	N = 25	154.3 (152.2, 157.7)	N = 18	0.209
Potassium (mmol/L)	3.80 (3.59, 4.06)	N = 25	4.35 (3.75, 4.73)	N = 18	0.003*
Chloride (mmol/L)	118.5 (116.2, 119.75)	N = 25	118.1 (116.6, 119.55)	N = 18	0.815
ALKP (U/L)	38 (31.5, 47)	N = 13	35 (29.5, 39)	N = 5	0.387
ALT (U/L)	44 (37, 55.25)	N = 14	48 (32, 99)	N = 5	0.622
AST (U/L)	28 (21.5, 31.5)	N = 13	26 (21.5, 34.5)	N = 5	0.849
USG	1.018 (1.013, 1.0305)	N = 30	1.0105 (1.009, 1.013)	N = 18	< 0.001**
UPC	0.1000 (0.0475, 0.2650)	N = 14	0.380 (0.075, 1.010)	N = 9	0.083

Difference between groups were evaluated using Mann–Whitney U test (continuous) or Chi-square (categorical).

Data are presented as median (IQR). * indicates $p < 0.05$. ** indicates $p < 0.001$.

Abbreviation: uHjv, urinary hemojuvelin; UHCR, urinary hemojuvelin-to-creatinine ratio; uMDA, urinary malondialdehyde; UMCR, urine malondialdehyde-to-creatinine ratio; BW, body weight; sCrea, serum creatinine; Sys BP, systolic arterial pressure; Hct, hematocrit; WBC, white blood cell count; A/G ratio, serum albumin-to-globulin ratio; BUN, blood urea nitrogen; ALKP, alkaline phosphatase; ALT, alanine aminotransferase; AST, aspartate aminotransferase; USG, urinary specific gravity; UPC, urine protein-to-creatinine ratio.

Simple logistic regression analysis showed sCrea, CKD sub-stage, uMDA, age, Hct, BUN, potassium and USG differed significantly between cats who progressed within 90 days and those who have not (sCrea, $p < 0.001$; uMDA, $p = 0.003$; age, $p = 0.002$; Hct, p

doi:10.6342/NTU202210133

= 0.008; BUN, p < 0.001; potassium, p = 0.003; USG, p < 0.001). UHCR and UMCR did not differ significantly (UHCR p = 0.101; UMCR p = 0.104).

Serum Crea, uMDA, age, Hct, BUN, potassium, and USG were enrolled into stepwise multiple logistic regression analysis; CKD sub-stage was not enrolled due to dependency with serum creatinine. BUN and uMDA were remained in the model, with p-value of 0.010 and 0.073, respectively (Table 4-7).

Table 4-7 Logistic regression analysis of 90-day progression and clinical parameters.

	Simple logistic regression			**Stepwise multiple logistic regression**		
Variables	OR	95% CI for OR	P value	OR	95% CI for OR	p-value
sCrea (mg/dL)	4.153	1.562-11.041	**0.004***			
CKD sub-stage	13.000	3.086-54.771	**< 0.001****			
uHjv (ng/mL)	1.138	0.911-1.421	0.256			
UHCR (10^{-7})	426.671	0.304-598566.388	0.101			
uMDA (ppb)	0.998	0.996-0.999	**0.008***	0.998	0.995-1.000	0.073
UMCR (ppb/mg/dL)	1.092	0.982-1.215	0.104			
Age (year)	1.230	1.069-1.415	**0.004***			
BW (kg)	0.830	0.483-1.425	0.499			
Sys BP (mmHg)	0.975	0.923-1.031	0.374			
Hct (%)	0.872	0.782-0.972	**0.013***			
WBC ($10^3/\mu$L)	1.000	1.000-1.000	0.211			
Alb (g/dL)	0.676	0.085-5.351	0.711			
Globulin (g/dL)	1.736	0.161-18.165	0.649			
A/G ratio	3.244	0.001-7499.695	0.766			
Glucose (mg/dL)	1.013	0.981-1.046	0.430			
BUN (mg/dL)	1.121	1.047-1.199	**0.001***	1.110	1.025-1.201	0.010*
Phos (mg/dL)	1.304	0.866-1.963	0.203			
Sodium (mmol/L)	0.811	0.710-1.094	0.252			
Potassium (mmol/L)	13.971	2.260-86.374	**0.005***			
Chloride (mmol/L)	0.975	0.800-1.189	0.804			
ALKP (U/L)	0.936	0.817-1.072	0.339			
ALT (U/L)	1.013	0.979-1.049	0.445			
AST (U/L)	0.995	0.865-1.146	0.949			
USG	$2.86*10^{-66}$	$1.45*10^{-116}$ -$5.65*10^{-16}$	**0.011***			
UPC	1.883	0.505-7.024	0.346			

doi:10.6342/NTU202210133

*Indicates $p < 0.05$. Bold font indicates $p < 0.1$ and enrollment into multiple logistic regression analysis.

Abbreviation: uHjv, urinary hemojuvelin; UHCR, urinary hemojuvelin-to-creatinine ratio; uMDA, urinary malondialdehyde; UMCR, urine malondialdehyde-to-creatinine ratio; BW, body weight; sCrea, serum creatinine; Sys BP, systolic arterial pressure; Hct, hematocrit; WBC, white blood cell count; A/G ratio, serum albumin-to-globulin ratio; BUN, blood urea nitrogen; ALKP, alkaline phosphatase; ALT, alanine aminotransferase; AST, aspartate aminotransferase; USG, urinary specific gravity; UPC, urine protein-to-creatinine ratio.

4.3.2 Receiver operating curve (ROC) for 90-day progression

To further analyze the prediction value of UHCR and UMCR to 90-day progression, ROC analysis was conducted. Under ROC analysis, UHCR showed significant predictive value for CKD progression, with an AUC of 0.728 ($p = 0.009$). The best cut-off, defined by maximizing the value of sensitivity plus specificity, was $47.744*10^{-7}$. The sensitivity and specificity for 90-day progression was 0.611 and 0.867, respectively (Figure 4-3).

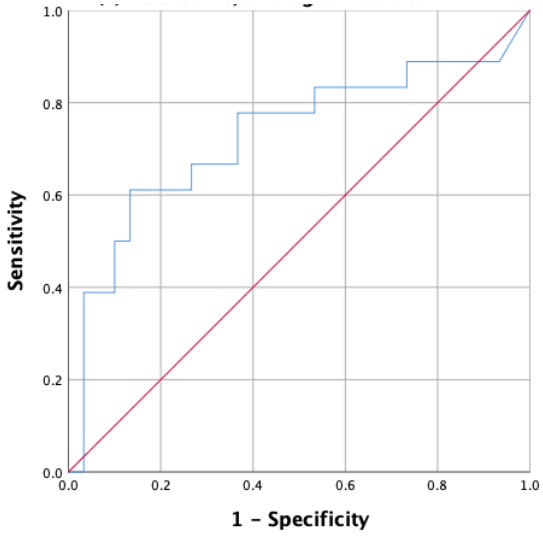

Figure 4-3 ROC curve for UHCR > $47.744*10^{-3}$ predicting progression within 90 days. 48 cases with recorded 90-day progression status were included. AUC = 0.728, p-value = 0.009. The best cut-off was $47.744*10^{-7}$, the sensitivity and specificity were 0.611 and 0.867, respectively.

doi:10.6342/NTU202210133

4.3.3 Survival analysis for CKD progression

To describe UHCR relation with CKD progression time, we established Kaplan-Meier (K-M) survival curve of all CKD cases. The endpoint was defined as CKD progression (serum creatinine elevation ≥ 0.5mg/dL). Cats were grouped into high-UHCR group or low-UHCR group using cut-off maximizing predictive value for 90-day progression (= 47.744 $*10^{-7}$).

Grouping by UHCR of 47.744 $*10^{-7}$ resulted in 40 cats in low-UHCR, 20 cats in high-UHCR group. K-M curve showed a significant difference in progression time between two groups, with p-value < 0.001. The estimated median progression time for low- and high-UHCR group was 556 days (95% CI, 246-866 days) and 81 days (95% CI, 40-122 days), respectively (Figure 4-4).

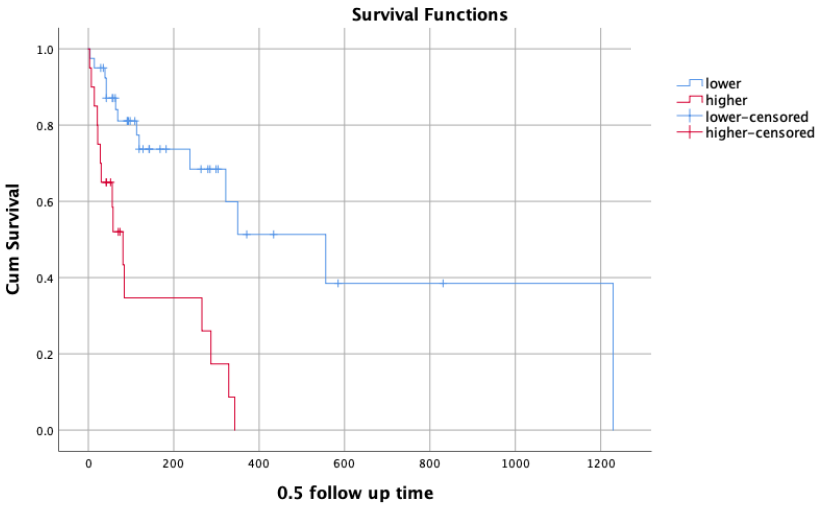

Figure 4-4 Kaplan-Meier survival curve for CKD progression, cases divided by UHCR of 47.744 $*10^{-7}$.

The estimated median progression time for low-UHCR group was 556 days (95% CI, 246-866 days); the estimated median progression time for high-UHCR group was 81 days (95% CI, 40-122 days). Log-rank test showed a significant difference in median survival time between groups (p-value, < 0.001).

doi:10.6342/NTU202210133

To verify the nature of UHCR predictive value on CKD progression time, we conducted Cox regression analysis to see whether this correlation can be explained by concurrent change of other clinical parameters. The results were summarized in Table 4-8.

In brief, the results showed a significant higher risk of progression in high-UHCR group. This increased risk is independent of age, sex, serum creatinine, BUN, globulin, A/G ratio, phosphorus, sodium and potassium.

Table 4-8 Cox regression analysis for CKD progression hazard ratio, cases divided by UHCR = 47.744 $*10^{-7}$.

Adjusting model	UHCR > 47.744*10^{-7}, HR	95% CI	p-value
(non)	4.337	1.971-9.545	< 0.001**
Model A	4.664	1.969-11.047	< 0.001**
Model B	3.489	1.467-8.297	0.005*
Model C	4.286	1.869-9.829	0.001*
Model D	3.622	1.578-8.311	0.002*
Model E	3.824	1.174-12.455	0.026*
Model F	3.839	1.182-12.467	0.025*
Model G	3.537	1.485-8.422	0.004*
Model H	3.554	1.597-7.909	0.002*
Model I	3.062	1.345-6.790	0.008*
Model J	2.732	1.122-6.656	0.027*
Model K	4.030	1.752-9.270	0.001*

* Indicates $p < 0.05$, ** indicated $p < 0.001$.

Model A = adjusted with age and sex; Model B = adjusted with sCrea and BUN; Model C = adjusted with BW; Model D = adjusted with Hct; Model E = adjusted with globulin; Model F = adjusted with A/G ratio; Model G = adjusted with phosphorus; Model H = adjusted for sodium; Model I = adjusted for potassium; Model J = adjusted for sCrea, BUN, and potassium; Model K, adjusted with UMCR.

Abbreviation: UHCR, urinary hemojuvelin-to-creatinine ratio; sCrea, serum creatinine; Hct, hematocrit; BUN, blood urea nitrogen; USG, urinary specific gravity; UPC, urine protein-to-creatinine ratio.

doi:10.6342/NTU202210133

Chapter 5 Discussion

To the best of our knowledge, this is the first study looking into the correlation between urinary Hjv and MDA in cats with naturally-occur CKD. Also, we investigated the prognostic value of creatinine-adjusted uHjv and uMDA in feline CKD.

5.1 UHCR and feline CKD progression

Our result showed a significant correlation between UHCR and feline CKD progression, whether within 90 days or throughout whole follow-up period. This predictive value is independent of age, traditional renal indexes (i.e., BUN and creatinine), globulin, and A/G ratio.

Renal disease is traditionally evaluated through indirect GFR markers, i.e., sCrea and BUN. Both markers are known to have low sensitivity, and unable to detect renal injury that does not affect GFR [4]. A more sensitive biomarker that can directly reflect renal tissue injury is therefore highly desirable. Hjv had been shown locally expressed in rats' and human kidneys, and its dysregulation links with multiple organs damage including kidneys [11, 14]. More specifically, urinary Hjv had been suggested reflecting renal local injury in both human and rats [11, 16, 17]. In people suffering from renal injury, uHjv elevates more promptly than sCrea, showing potential to be a more sensitive marker for renal disease [16, 17].

Although uHjv was previously studied under the context of AKI in human and rats, uHjv of CKD cats had shown an elevation comparable to that of AKI [18]. Additionally, an intimate link had been proposed between AKI and CKD [88], and several kidney injury biomarkers originally identified in AKI had been found to be predictive for CKD progression in human, dogs, and cats [4, 88]. Taken together, uHjv seems promising to

doi:10.6342/NTU202210133

serve as a new biomarker for feline CKD, able to directly reflect renal tissue injury and detect renal disease in an earlier stage.

The mHjv-hepcidin axis had been shown to protect kidneys from local iron deposition [11]. People with CKD is known to have a conflicting iron status, showing systemic iron deficiency and local renal iron overload [9], while the latter contributes to renal injury in both human and rats [6-8]. However, reports on iron status in CKD cats had been focusing extensively on systemic iron deficiency, with minimal address on renal iron accumulation [80, 89-91]. Recently, our team had showed an increased uHjv in cats with renal disease [18], indicating a link between iron and renal damage similar to that in people and rats. A further look into the tissue-specific iron status is therefore highly warrant, especially as iron supplementation is frequently used to address systemic iron deficiency in these patients.

5.2 The correlation between UHCR and UMCR in CKD cats

Our study found a significant positive correlation between UHCR and UMCR. This correlation is independent traditional renal function indexes (i.e., sCrea and BUN) along with other clinical parameters, but possibly related to a concurrent change of serum globulin.

As above mentioned, mHjv cleavage and subsequently down-regulation of the mHjv-hepcidin axis results in renal iron deposition [11]. Iron catalyze lipid oxidation [82]; therefore, cleavage of mHjv on kidney cells is likely to cause renal lipid peroxidation, represented by UMCR, and concurrent sHjv release into urine, represented by UHCR.

Additionally, iron contributes to CKD inflammation [6-9, 33]. Inflammation and oxidative stress are known to be interdependent pathophysiological processes [92]. uHjv

doi:10.6342/NTU202210133

and iron accumulation can therefore also link to renal MDA production through inflammation. This hypothesis can be supported by the fact that globulin, an indicator for inflammation, change concurrently with UHCR and UMCR.

Last but not least, iron accumulation can lead to a newly-described form of cell death, known as ferroptosis. This kind of cell death is featured by lipid peroxidation, and had been shown contributes to various types of kidney injuries in rats and human [9, 34, 36]. Correlation between UHCR and UMCR in CKD cats may indicate ferroptosis also play a role in renal disease of this species, which warrant a further investigation through ferroptosis-specific biomarkers.

5.3 Urinary Hjv and other clinical parameters in CKD cats

In the present study, UHCR showed a significant negative correlation with USG, and a positive correlation with BUN. However, we did not find a significant correlation between UHCR and sCrea, despite UHCR was higher in late-stage CKD compared to that in early stage.

sCrea evaluate kidney status through indirectly reflecting renal GFR [4]. On the other hand, Hjv dysregulation and increased urine Hjv concentration is purposed linking to renal tissue damage in rats and human, as above mentioned [11, 16, 17]. We suggested that UHCR may also reflect cats' renal tissue injury. As renal injury may not be represented with the change of GFR [4], UHCR may failed to correlate with sCrea, since they evaluate kidney disease from different aspects.

BUN is traditionally viewed as an indirect GFR marker in kidney diseases. However, it was recently shown that BUN is associated with adverse renal outcome (i.e., dialysis or death) in human CKD, independent to estimated GFR [93]. This indicates that BUN also

doi:10.6342/NTU202210133

correlates with renal disease through mechanism other than GFR. The exact mechanism is currently unclear, but purposed related the tissue toxicity of urea or its dissociation product, isocyanate [93]. Our finding that BUN was the independent parameter to influence UHCR indicates that renal injury caused by BUN may also lead to UHCR elevation.

5.4 Urinary MDA and other clinical parameters in CKD cats

Surprisingly, we found no significant relation between UMCR and CKD progression. Oxidative stress is a well-described pathologic factor for renal diseases, and Plasma MDA had been found to correlated with CKD severity in human patients [25-27].

However, a profound difference likely to exist between human and cats regarding the oxidative stress status during CKD [73]. Reduced-to-oxidated-glutathione ratio, an indicator for renal anti-oxidant capacity, was decreased in human CKD, but elevated in feline CKD [94]. Moreover, the serum glutathione peroxidase activity, which indicates body anti-oxidative ability, was found to be higher in cats with stage 4 CKD compared to healthy cats. This also contradicted studies in human CKD [95]. Together, these findings may indicate a difference between human and feline oxidation status during CKD, leading to different oxidative indicators patterns [73, 94, 95].

UMCR showed an independent positive correlation with serum potassium. Declined GFR had been linked to hyperkalemia in both general population [96] and patients with CKD [97], proposed due to decreased urinary excretion. The positive correlation between UMCR and serum potassium can therefore indicate a correlation still exist between UMCR and GFR, despite this change of GFR failed to reflect on sCrea.

doi:10.6342/NTU202210133

5.5 Limitations

Our study has several limitations. First, the retrospective nature of the study limited our ability to obtained complete clinical parameters in every cases. Some parameter of potential importance, ex. urine protein-to-creatinine ratio, failed to build significant regression model under multiple Cox regression analysis due to small sample size. Retrospective design also limits us from obtaining complete records of several clinical settings potentially important for our results, including body condition score, diet, iron supplementation, and a standardized evaluation of hydration status. Also, we did not include control group to allow comparison between healthy and diseased cats. However, our team had previously evaluated difference between healthy and CKD cats, on both UHCR [18] and UMCR (Chang et al. 2021, unpublished data). Considering limited sample volume, a repeated evaluation of healthy control was not deemed necessary. Finally, urine soluble Hjv will be most ideally interpreted along with membranous Hjv in kidney tissue. This, however, will require a tissue biopsy, which is not practical to obtain for most client-own cases.

5.6 Conclusions

UHCR showed a significant prognostic value for feline CKD progression independent of traditional renal indexes (i.e., BUN and creatinine). Meanwhile, UMCR did not predict CKD progression, but correlated significantly with UHCR. Therefore, UHCR-related iron dysregulation may deteriorate CKD partially through lipid oxidation in cats.

doi:10.6342/NTU202210133

References

1. Brown, C.A., et al., *Chronic Kidney Disease in Aged Cats: Clinical Features, Morphology, and Proposed Pathogeneses.* Vet Pathol, 2016. **53**(2): p. 309-26.
2. Reynolds, B.S. and H.P. Lefebvre, *Feline CKD:Pathophysiology and risk factors — what do we know?* Journal of Feline Medicine and Surgery, 2013. **15**(1_suppl): p. 3-14.
3. Sparkes, A.H., et al., *ISFM Consensus Guidelines on the Diagnosis and Management of Feline Chronic Kidney Disease.* J Feline Med Surg, 2016. **18**(3): p. 219-39.
4. Kongtasai, T., et al., *Renal biomarkers in cats: A review of the current status in chronic kidney disease.* J Vet Intern Med, 2022. **36**(2): p. 379-396.
5. Quimby, J., et al., *Renal Senescence, Telomere Shortening and Nitrosative Stress in Feline Chronic Kidney Disease.* Vet Sci, 2021. **8**(12).
6. van Swelm, R.P.L., J.F.M. Wetzels, and D.W. Swinkels, *The multifaceted role of iron in renal health and disease.* Nat Rev Nephrol, 2020. **16**(2): p. 77-98.
7. Ikeda, Y., et al., *Dietary iron restriction alleviates renal tubulointerstitial injury induced by protein overload in mice.* Sci Rep, 2017. **7**(1): p. 10621.
8. Ikeda, Y., et al., *Dietary iron restriction inhibits progression of diabetic nephropathy in db/db mice.* Am J Physiol Renal Physiol, 2013. **304**(7): p. F1028-36.
9. Wang, J., et al., *Ferroptosis, a new target for treatment of renal injury and fibrosis in a 5/6 nephrectomy-induced CKD rat model.* Cell Death Discov, 2022. **8**(1): p. 127.
10. Malyszko, J., et al., *Is hemojuvelin a possible new player in iron metabolism in hemodialysis patients?* Int Urol Nephrol, 2012. **44**(6): p. 1805-11.
11. Young, G.H., et al., *Hemojuvelin modulates iron stress during acute kidney injury: improved by furin inhibitor.* Antioxid Redox Signal, 2014. **20**(8): p. 1181-94.
12. Luciani, N., et al., *Hemojuvelin: a new link between obesity and iron homeostasis.* Obesity (Silver Spring), 2011. **19**(8): p. 1545-51.
13. Agarwal, A.K. and J. Yee, *Hepcidin.* Adv Chronic Kidney Dis, 2019. **26**(4): p. 298-305.
14. Zhang, A.S., *Control of systemic iron homeostasis by the hemojuvelin-hepcidin axis.* Adv Nutr, 2010. **1**(1): p. 38-45.
15. Ferro, E., et al., *Soluble hemojuvelin in transfused and untransfused thalassaemic subjects.* Eur J Haematol, 2017. **98**(1): p. 67-74.
16. Wang, J.J., et al., *Urinary biomarkers predict advanced acute kidney injury after cardiovascular surgery.* Crit Care, 2018. **22**(1): p. 108.
17. Ko, S.W., et al., *Hemojuvelin Predicts Acute Kidney Injury and Poor Outcomes Following Cardiac Surgery.* Sci Rep, 2018. **8**(1): p. 1938.
18. Jing, H., et al., *Urine hemojuvelin in cats with naturally occurring kidney disease.* J Vet Intern Med, 2020. **34**(3): p. 1222-1230.
19. Bayraktar, A., et al., *The Effect of Hepcidin on Cardiac Ischemia-Reperfusion Injury.* J Invest Surg, 2020. **33**(9): p. 813-821.
20. Schwartz, A.J., et al., *Hepcidin sequesters iron to sustain nucleotide metabolism and mitochondrial function in colorectal cancer epithelial cells.* Nat Metab, 2021. **3**(7): p. 969-982.
21. Folgueras, A.R., et al., *Matriptase-2 deficiency protects from obesity by*

doi:10.6342/NTU202210133

modulating iron homeostasis. Nat Commun, 2018. **9**(1): p. 1350.
22. Tsikas, D., *Assessment of lipid peroxidation by measuring malondialdehyde (MDA) and relatives in biological samples: Analytical and biological challenges*. Anal Biochem, 2017. **524**: p. 13-30.
23. Liu, D., et al., *Using inflammatory and oxidative biomarkers in urine to predict early acute kidney injury in patients undergoing liver transplantation.* Biomarkers, 2014. **19**(5): p. 424-9.
24. Hodovanets, Y., et al., *URINARY MALONDIALDEHYDE AS A PREDICTIVE AND DIAGNOSTIC MARKER FOR NEONATAL ACUTE KIDNEY INJURY.* Georgian Med News, 2018(278): p. 126-132.
25. Vida, C., et al., *Oxidative Stress in Patients with Advanced CKD and Renal Replacement Therapy: The Key Role of Peripheral Blood Leukocytes.* Antioxidants (Basel), 2021. **10**(7).
26. Tomas-Simo, P., et al., *Oxidative Stress in Non-Dialysis-Dependent Chronic Kidney Disease Patients.* Int J Environ Res Public Health, 2021. **18**(15).
27. Li, G., et al., *Association between age-related decline of kidney function and plasma malondialdehyde.* Rejuvenation Res, 2012. **15**(3): p. 257-64.
28. Yu, S. and I. Paetau-Robinson, *Dietary supplements of vitamins E and C and beta-carotene reduce oxidative stress in cats with renal insufficiency.* Vet Res Commun, 2006. **30**(4): p. 403-13.
29. Valle, E., et al., *Investigation of hallmarks of carbonyl stress and formation of end products in feline chronic kidney disease as markers of uraemic toxins.* Journal of Feline Medicine and Surgery, 2018. **21**(6): p. 465-474.
30. McCown, J.L. and A.J. Specht, *Iron homeostasis and disorders in dogs and cats: a review.* J Am Anim Hosp Assoc, 2011. **47**(3): p. 151-60.
31. Tucker, P.S., A.T. Scanlan, and V.J. Dalbo, *Chronic kidney disease influences multiple systems: describing the relationship between oxidative stress, inflammation, kidney damage, and concomitant disease.* Oxid Med Cell Longev, 2015. **2015**: p. 806358.
32. Weiss, A., et al., *Orchestrated regulation of iron trafficking proteins in the kidney during iron overload facilitates systemic iron retention.* PLoS One, 2018. **13**(10): p. e0204471.
33. Bochi, G.V., et al., *Fenton Reaction-Generated Advanced Oxidation Protein Products Induces Inflammation in Human Embryonic Kidney Cells.* Inflammation, 2016. **39**(4): p. 1285-90.
34. Wang, J., et al., *The Cross-Link between Ferroptosis and Kidney Diseases.* Oxid Med Cell Longev, 2021. **2021**: p. 6654887.
35. Belavgeni, A., et al., *Ferroptosis and Necroptosis in the Kidney.* Cell Chem Biol, 2020. **27**(4): p. 448-462.
36. Linkermann, A., et al., *Synchronized renal tubular cell death involves ferroptosis.* Proc Natl Acad Sci U S A, 2014. **111**(47): p. 16836-41.
37. Friedmann Angeli, J.P., et al., *Inactivation of the ferroptosis regulator Gpx4 triggers acute renal failure in mice.* Nat Cell Biol, 2014. **16**(12): p. 1180-91.
38. Nakayama, M., et al., *A case of IgA nephropathy and renal hemosiderosis associated with primary hemochromatosis.* Ren Fail, 2008. **30**(8): p. 813-7.
39. Ozkurt, S., et al., *Renal hemosiderosis and rapidly progressive glomerulonephritis associated with primary hemochromatosis.* Ren Fail, 2014. **36**(5): p. 814-6.
40. Moulouel, B., et al., *Hepcidin regulates intrarenal iron handling at the distal nephron.* Kidney Int, 2013. **84**(4): p. 756-66.

doi:10.6342/NTU202210133

41. Probst, S., et al., *Role of hepcidin in oxidative stress and cell death of cultured mouse renal collecting duct cells: protection against iron and sensitization to cadmium.* Arch Toxicol, 2021. **95**(8): p. 2719-2735.
42. Norden, A.G., et al., *Glomerular protein sieving and implications for renal failure in Fanconi syndrome.* Kidney Int, 2001. **60**(5): p. 1885-92.
43. Vilasi, A., et al., *Combined proteomic and metabonomic studies in three genetic forms of the renal Fanconi syndrome.* Am J Physiol Renal Physiol, 2007. **293**(2): p. F456-67.
44. Kovac, S., et al., *Anti-hemojuvelin antibody corrects anemia caused by inappropriately high hepcidin levels.* Haematologica, 2016. **101**(5): p. e173-6.
45. Krijt, J., et al., *Matriptase-2 and Hemojuvelin in Hepcidin Regulation: In Vivo Immunoblot Studies in Mask Mice.* Int J Mol Sci, 2021. **22**(5).
46. Silvestri, L., et al., *The serine protease matriptase-2 (TMPRSS6) inhibits hepcidin activation by cleaving membrane hemojuvelin.* Cell Metab, 2008. **8**(6): p. 502-11.
47. Rumjon, A., et al., *Serum hemojuvelin and hepcidin levels in chronic kidney disease.* Am J Nephrol, 2012. **35**(3): p. 295-304.
48. Noels, H., et al., *Lipoproteins and fatty acids in chronic kidney disease: molecular and metabolic alterations.* Nat Rev Nephrol, 2021. **17**(8): p. 528-542.
49. Baek, J., et al., *Lipidomic approaches to dissect dysregulated lipid metabolism in kidney disease.* Nat Rev Nephrol, 2022. **18**(1): p. 38-55.
50. Bermudez-Lopez, M., et al., *New perspectives on CKD-induced dyslipidemia.* Expert Opin Ther Targets, 2017. **21**(10): p. 967-976.
51. Hager, M.R., A.D. Narla, and L.R. Tannock, *Dyslipidemia in patients with chronic kidney disease.* Rev Endocr Metab Disord, 2017. **18**(1): p. 29-40.
52. Brunetto, M.A., et al., *Healthy and Chronic Kidney Disease (CKD) Dogs Have Differences in Serum Metabolomics and Renal Diet May Have Slowed Disease Progression.* Metabolites, 2021. **11**(11).
53. Behling-Kelly, E., *Serum lipoprotein changes in dogs with renal disease.* J Vet Intern Med, 2014. **28**(6): p. 1692-8.
54. Gyebi, L., Z. Soltani, and E. Reisin, *Lipid nephrotoxicity: new concept for an old disease.* Curr Hypertens Rep, 2012. **14**(2): p. 177-81.
55. Cases, A. and E. Coll, *Dyslipidemia and the progression of renal disease in chronic renal failure patients.* Kidney Int Suppl, 2005(99): p. S87-93.
56. Hsu, C.Y., et al., *Diabetes, hemoglobin A(1c), cholesterol, and the risk of moderate chronic renal insufficiency in an ambulatory population.* Am J Kidney Dis, 2000. **36**(2): p. 272-81.
57. Fox, C.S., et al., *Predictors of new-onset kidney disease in a community-based population.* Jama, 2004. **291**(7): p. 844-50.
58. Florens, N., et al., *Modified Lipids and Lipoproteins in Chronic Kidney Disease: A New Class of Uremic Toxins.* Toxins (Basel), 2016. **8**(12).
59. Kang, H.M., et al., *Defective fatty acid oxidation in renal tubular epithelial cells has a key role in kidney fibrosis development.* Nat Med, 2015. **21**(1): p. 37-46.
60. Han, S.H., et al., *PGC-1alpha Protects from Notch-Induced Kidney Fibrosis Development.* J Am Soc Nephrol, 2017. **28**(11): p. 3312-3322.
61. Miguel, V., et al., *Renal tubule Cpt1a overexpression protects from kidney fibrosis by restoring mitochondrial homeostasis.* J Clin Invest, 2021. **131**(5).
62. Martino-Costa, A.L., et al., *Renal Interstitial Lipid Accumulation in Cats with Chronic Kidney Disease.* J Comp Pathol, 2017. **157**(2-3): p. 75-79.
63. McLeland, S.M., et al., *A comparison of biochemical and histopathologic staging*

doi:10.6342/NTU202210133

in cats with chronic kidney disease. Vet Pathol, 2015. **52**(3): p. 524-34.
64. Schmiedt, C.W., et al., *Unilateral Renal Ischemia as a Model of Acute Kidney Injury and Renal Fibrosis in Cats.* Vet Pathol, 2016. **53**(1): p. 87-101.
65. Bargmann, W., et al., *Lipids in the proximal convoluted tubule of the cat kidney and the reabsorption of cholesterol.* Cell and Tissue Research, 1977. **177**(4): p. 523-538.
66. Schwarz, T., et al., *CT features of feline lipiduria and renal cortical lipid deposition.* J Feline Med Surg, 2021. **23**(4): p. 357-363.
67. Daenen, K., et al., *Oxidative stress in chronic kidney disease.* Pediatr Nephrol, 2019. **34**(6): p. 975-991.
68. Duni, A., et al., *Oxidative Stress in the Pathogenesis and Evolution of Chronic Kidney Disease: Untangling Ariadne's Thread.* Int J Mol Sci, 2019. **20**(15).
69. Gyuraszova, M., et al., *Oxidative Stress in the Pathophysiology of Kidney Disease: Implications for Noninvasive Monitoring and Identification of Biomarkers.* Oxid Med Cell Longev, 2020. **2020**: p. 5478708.
70. Moradi, H., et al., *Impaired antioxidant activity of high-density lipoprotein in chronic kidney disease.* Transl Res, 2009. **153**(2): p. 77-85.
71. Pieniazek, A., J. Bernasinska-Slomczewska, and L. Gwozdzinski, *Uremic Toxins and Their Relation with Oxidative Stress Induced in Patients with CKD.* Int J Mol Sci, 2021. **22**(12).
72. Ruggiero, C., et al., *Albumin-bound fatty acids but not albumin itself alter redox balance in tubular epithelial cells and induce a peroxide-mediated redox-sensitive apoptosis.* Am J Physiol Renal Physiol, 2014. **306**(8): p. F896-906.
73. Whitehouse, W., et al., *Urinary F2 -Isoprostanes in Cats with International Renal Interest Society Stage 1-4 Chronic Kidney Disease.* J Vet Intern Med, 2017. **31**(2): p. 449-456.
74. Gonzalez-Dominguez, A., et al., *Iron Metabolism in Obesity and Metabolic Syndrome.* Int J Mol Sci, 2020. **21**(15).
75. Alshwaiyat, N.M., et al., *Association between obesity and iron deficiency (Review).* Exp Ther Med, 2021. **22**(5): p. 1268.
76. Miricescu, D., et al., *Impact of adipose tissue in chronic kidney disease development (Review).* Exp Ther Med, 2021. **21**(5): p. 539.
77. Martos-Rus, C., et al., *Macrophage and adipocyte interaction as a source of inflammation in kidney disease.* Sci Rep, 2021. **11**(1): p. 2974.
78. Wang, C., et al., *A high-fructose diet in rats induces systemic iron deficiency and hepatic iron overload by an inflammation mechanism.* J Food Biochem, 2021. **45**(1): p. e13578.
79. Citelli, M., et al., *Obesity promotes alterations in iron recycling.* Nutrients, 2015. **7**(1): p. 335-48.
80. Javard, R., et al., *Acute-Phase Proteins and Iron Status in Cats with Chronic Kidney Disease.* J Vet Intern Med, 2017. **31**(2): p. 457-464.
81. Coimbra, S., C. Catarino, and A. Santos-Silva, *The role of adipocytes in the modulation of iron metabolism in obesity.* Obes Rev, 2013. **14**(10): p. 771-9.
82. Forcina, G.C. and S.J. Dixon, *GPX4 at the Crossroads of Lipid Homeostasis and Ferroptosis.* Proteomics, 2019. **19**(18): p. e1800311.
83. Plotnikov, E.Y., et al., *Myoglobin causes oxidative stress, increase of NO production and dysfunction of kidney's mitochondria.* Biochim Biophys Acta, 2009. **1792**(8): p. 796-803.
84. Song, S.J., et al., *Rhabdomyolysis-Induced AKI Was Ameliorated in NLRP3 KO*

doi:10.6342/NTU202210133

Mice via Alleviation of Mitochondrial Lipid Peroxidation in Renal Tubular Cells. Int J Mol Sci, 2020. **21**(22).
85. Merle, U., et al., *The iron regulatory peptide hepcidin is expressed in the heart and regulated by hypoxia and inflammation.* Endocrinology, 2007. **148**(6): p. 2663-8.
86. Grotto, D., et al., *Importance of the lipid peroxidation biomarkers and methodological aspects FOR malondialdehyde quantification.* Quím. Nova. **32**(1): p. 169-174.
87. Mendes, R., C. Cardoso, and C. Pestana, *Measurement of malondialdehyde in fish: A comparison study between HPLC methods and the traditional spectrophotometric test.* Food Chemistry, 2009. **112**(4): p. 1038-1045.
88. Cowgill, L.D., et al., *Is Progressive Chronic Kidney Disease a Slow Acute Kidney Injury?* Vet Clin North Am Small Anim Pract, 2016. **46**(6): p. 995-1013.
89. Betting, A., A. Schweighauser, and T. Francey, *Diagnostic value of reticulocyte indices for the assessment of the iron status of cats with chronic kidney disease.* J Vet Intern Med, 2022. **36**(2): p. 619-628.
90. Chalhoub, S., C. Langston, and A. Eatroff, *Anemia of renal disease: what it is, what to do and what's new.* J Feline Med Surg, 2011. **13**(9): p. 629-40.
91. Gest, J., C. Langston, and A. Eatroff, *Iron Status of Cats with Chronic Kidney Disease.* J Vet Intern Med, 2015. **29**(6): p. 1488-93.
92. Samsu, N. and M.I. Bellini, *Diabetic Nephropathy: Challenges in Pathogenesis, Diagnosis, and Treatment.* BioMed Research International, 2021. **2021**: p. 1-17.
93. Seki, M., et al., *Blood urea nitrogen is independently associated with renal outcomes in Japanese patients with stage 3-5 chronic kidney disease: a prospective observational study.* BMC Nephrol, 2019. **20**(1): p. 115.
94. Keegan, R.F. and C.B. Webb, *Oxidative stress and neutrophil function in cats with chronic renal failure.* J Vet Intern Med, 2010. **24**(3): p. 514-9.
95. Krofic Zel, M., N. Tozon, and A. Nemec Svete, *Plasma and erythrocyte glutathione peroxidase activity, serum selenium concentration, and plasma total antioxidant capacity in cats with IRIS stages I-IV chronic kidney disease.* J Vet Intern Med, 2014. **28**(1): p. 130-6.
96. Palaka, E., et al., *Associations between serum potassium and adverse clinical outcomes: A systematic literature review.* Int J Clin Pract, 2020. **74**(1): p. e13421.
97. Valdivielso, J.M., et al., *Hyperkalemia in Chronic Kidney Disease in the New Era of Kidney Protection Therapies.* Drugs, 2021. **81**(13): p. 1467-1489.

doi:10.6342/NTU202210133